



Title	pH-dependent leaching of arsenic from shield-tunneling excavated soils and its countermeasures
Author(s)	Ho, Gia Duc
Citation	北海道大学. 博士(工学) 甲第14454号
Issue Date	2021-03-25
DOI	10.14943/doctoral.k14454
Doc URL	<a href="http://hdl.handle.net/2115/84454">http://hdl.handle.net/2115/84454</a>
Type	theses (doctoral)
File Information	Ho_Gia_Duc.pdf



[Instructions for use](#)

**pH-dependent leaching of arsenic from shield-tunneling excavated soils  
and its countermeasures**

A dissertation submitted in partial fulfillment of the  
requirements for the degree of Doctorate in  
Engineering

By

**HO GIA DUC**



Division of Sustainable Resources Engineering  
Graduate School of Engineering,  
Hokkaido University, Japan

2021

## ABSTRACT

Underground facilities have become common in most developed countries. In recent years, it is also becoming more common in developing countries to fulfill the demand of utilization of underground space due to rapid population growth and urbanization. A number of various purposes of using underground facilities such as subway, new bullet/high speed train routes, hydro-electric powerplants, shopping malls, parking spaces and sewer/utility systems have been reported. In order to build these kinds of facilities, tunnel excavation is important and the first step. Meanwhile, tunnel construction in soft alluvial deposits is generally done using the shield-tunneling method, a technique that requires the mixing of cementitious materials with excavated soils to reinforce and stabilize the excavated tunnel walls. Although the mechanical properties of soft soils and sediments are improved after introduction of cementitious materials, this process could increase the pH of these geological materials and mobilize naturally occurring arsenic (As). In other words, shield-tunneling excavation could create favorable conditions for As leaching. However, how cementitious materials addition releases As from shield-tunneling excavated soils is not well understood. In the present study, therefore, the effects of cement addition on As leaching from the excavated soils were clarified. Understanding As leaching behaviors helps better finding out the solution against As leaching. The countermeasures of As leaching by adding adsorbents were then investigated. Finally, the outcomes of the present study provide helpful information on management of these alkaline excavated soils. The dissertation contains five chapters.

In chapter 1, As contamination in soils, geochemistry of As in environments, the removal of As, and shield-tunneling excavation are briefly reviewed and introduced.

There have been a number of publications on the characteristics of As leaching from soils, rocks, or industrial wastes. However, these studies focused on soils, rocks, or materials other than shield-tunneling excavated soils, or the characteristics of As leaching from rocks/soils versus pH by changing the pH with hydrochloric acid (HCl) and sodium hydroxide (NaOH). In other words, the effects of pH on As leaching from shield-tunneling excavated soils by cement addition is not well understood. Therefore, chapter 2—literature review chapter—will give a brief summary of the recent studies

regarding the As leaching characteristics, and the necessities and the objectives of the present study are then depicted.

In chapter 3, the effects of cement addition on As leaching from tunnel-excavated soils naturally contaminated with As were investigated. Sequential extraction experiments were also carried out to determine the chemical forms, solid-phase partitioning and leachability of As in the soils. In the absence of cement, sequential extraction showed higher As leaching from the soils when the exchangeable As fraction and total As content increased. In contrast, As leaching increased up to pH 10.3 and then decreased at higher pH values when cement was added. This trend was observed irrespective of the soil samples, which indicates that pH adjustment is an important countermeasure in restricting As leaching from excavated soils. The results of attenuated total reflectance Fourier transform infrared spectroscopy (ATR-FTIR) showed slight changes in the chemical properties of soils due to cement addition but the chemical phases of As remained unchanged.

After identifying the effects of cement addition on As leaching from soils excavated by the shield-tunneling method, the countermeasures against As leaching should carefully be considered, which was presented in Chapter 4. One of the convenient methods is to add an adsorbent. Among potential adsorbents, magnesium oxide (MgO), half-burnt dolomite (MgO.CaCO<sub>3</sub>), and iron oxide (Fe<sub>2</sub>O<sub>3</sub>) are considered as economical and easily available adsorbents. However, their performance on removal of As released from the soils is not well understood. Therefore, the performance of the adsorbents was evaluated by leaching experiments. The results showed that all of the adsorbents used at the ratio of less than 1% compared with soil worked effectively in restricting As leaching and that the performance of the three adsorbents was almost the same. These imply that As leaching is restricted by adding the adsorbents. ATR-FTIR was also applied to observe the changes in chemical bonding of soil with and without adsorbents. The results showed that a slight change in the chemical bonding of soil was detected in case of half-burnt dolomite addition whereas that in case of magnesium oxide and iron oxide addition remained unchanged.

Chapter 5 summarizes all general conclusions of the present study. The results could provide the fundamental knowledge of the management of these alkaline excavated soils.

## CONTENTS

LIST OF FIGURES .....	vii
LIST OF TABLES .....	ix
CHAPTER 1 .....	1
GENERAL INTRODUCTION.....	1
1.1 Arsenic contamination in soils.....	1
1.2 Geochemistry of arsenic in environments.....	2
1.3 The removal of arsenic .....	2
1.4 Shield-tunneling excavation .....	4
References.....	5
CHAPTER 2 .....	7
LITERATURE REVIEW .....	7
2.1 The recent studies regarding the As leaching characteristics.....	7
2.2 Statement of the problem and objectives of the study .....	10
2.3 Outline of dissertation.....	10
References.....	12
CHAPTER 3 .....	15
EFFECTS OF CEMENT ADDITION ON ARSENIC LEACHING FROM SOILS EXCAVATED FROM PROJECTS EMPLOYING SHIELD-TUNNELING METHOD .....	15
3.1 Introduction .....	15
3.2 Materials and Methods .....	16
3.2.1 Characterization of soil samples .....	16
3.2.2 Batch leaching experiments .....	17
3.2.3 Sequential extraction.....	19
3.3 Results and Discussion .....	20
3.3.1 Properties of soil samples .....	20
3.3.2 Batch leaching experiments without cement addition.....	21
3.3.3 Batch leaching experiments with cement addition.....	24
3.3.4 Sequential extraction without cement .....	27
3.3.5 Sequential extraction with cement addition .....	29
3.4 Conclusion .....	32

References.....	34
CHAPTER 4.....	42
EFFECTS OF ADSORBENTS ADDITION ON ARSENIC LEACHING FROM SHIELD-TUNNELING EXCAVATED SOILS .....	42
4.1 Introduction .....	42
4.2 Materials and methods.....	43
4.2.1 Materials used .....	43
4.2.1.1 Soil samples .....	43
4.2.1.2 Cement .....	43
4.2.1.3 Adsorbent.....	44
4.2.1.3 Foam reagent and coagulant .....	44
4.2.2 Batch leaching experiments .....	44
4.2.2.1 Batch leaching experiments without adsorbent.....	44
4.2.2.2 Batch leaching experiments with adsorbent.....	48
4.2.2.3 Batch leaching experiments with foam reagent and coagulant .....	48
4.2.3 Characterization of soil samples .....	49
4.2.4 Saturation index calculations .....	49
4.2.5 Geochemist’s Workbench® model.....	49
4.2.6 Principle component analysis (PCA) .....	50
4.3 Results and discussion .....	50
4.3.1 Properties of soil samples .....	50
4.3.2 Batch leaching experiments with adsorbent.....	51
4.3.2.1 Batch leaching experiments with magnesium oxide .....	51
4.3.2.2 Batch leaching experiments with half burnt-dolomite .....	56
4.3.2.3 Batch leaching experiments with iron oxide.....	59
4.3.3 Performance of adsorbents.....	63
4.3.4 Changes in properties of soil samples with and without adsorbents.....	66
4.3.5 Batch leaching experiments with foam reagent and coagulant .....	67
References.....	70
CHAPTER 5.....	75

GENERAL CONCLUSION .....	75
ACKNOWLEDGMENT.....	77

## LIST OF FIGURES

<b>Fig. 1.1.</b> Arsenic distribution in Hokkaido.....	1
<b>Fig. 1.2.</b> Generalized geochemical cycle of arsenic (Boyle and Jonasson, 1973).....	3
<b>Fig. 1.3.</b> Eh-pH diagram of As species for an As-O <sub>2</sub> -H <sub>2</sub> O system at 25°C and 1 bar.....	4
<b>Fig. 2.1.</b> As leaching concentration from hydrothermally altered igneous rocks as a function of pH under oxic conditions (Tabelin and Igarashi, 2009) .....	7
<b>Fig. 2.2.</b> Leaching behaviors of As from sedimentary rocks as a function of pH (Tabelin et al., 2014a) .....	8
<b>Fig. 2.3.</b> Changes in pH and arsenic solubility in samples 1, 2 and 3, as affected by various doses of HCl and NaOH. Doses are expressed in cm <sup>3</sup> of 1 mol/dm <sup>3</sup> HCl or 1 mol/dm <sup>3</sup> NaOH per 5 g soil. Arsenic release is illustrated in mg/kg (A) and as a percentage of the total arsenic in soils (B) (Gersztyn et al., 2013).....	9
<b>Fig. 3.1.</b> Leaching concentration of As from soils without cement addition .....	21
<b>Fig. 3.2.</b> The changes in leaching concentration of As versus pH with and without cement addition .....	24
<b>Fig. 3.3.</b> Eh-pH predominance diagram of As at 25°C, 1.013 bar, activity of As = 10 <sup>-6</sup> , activity of SO <sub>4</sub> <sup>2-</sup> = 10 <sup>-3</sup> and activity of Ca <sup>2+</sup> = 10 <sup>-4</sup> . The diagram was created using the Geochemist's Workbench®. .....	26
<b>Fig. 3.4.</b> Schematic diagrams of As adsorption with and without cement.....	26
<b>Fig. 3.5.</b> Results of sequential extraction of original soil samples.....	27
<b>Fig. 3.6.</b> Positive correlation between As leaching concentration and exchangeable As content .....	28
<b>Fig. 3.7.</b> Positive correlation between As leaching concentration and total As content	28
<b>Fig. 3.8.</b> Sequential extraction of Sample D without cement and with cement at 0.3 and 1.5% of soil.....	29
<b>Fig. 3.9.</b> Positive correlations of leaching concentrations of SO <sub>4</sub> <sup>2-</sup> (a), Si (b), and Ca (c) and pH .....	30
<b>Fig. 3.10.</b> The changes in zeta potential versus pH of Sample A (a), Sample D (b), and Sample F (c) with and without cement.....	31
<b>Fig. 3.11.</b> The changes in ATR-FTIR of Sample D with and without cement, absorption bands (a) from 3,000 to 4,000 (cm <sup>-1</sup> ), (b) from 1,200 to 3,000 (cm <sup>-1</sup> ), and (c) from 400 to 1,200 (cm <sup>-1</sup> ) .....	32
<b>Fig. 4.1.</b> The composed minerals of samples A, D, and F with and without cement addition.....	51
<b>Fig. 4.2.</b> Effects of addition of magnesium oxide on As leaching .....	52
<b>Fig. 4.3.</b> Leaching concentration of Mg <sup>2+</sup> versus the amount of magnesium oxide addition.....	53



<b>Fig. 4.4.</b> Schematic diagram of As adsorption/precipitation/co-precipitation on magnesium oxide and half-burnt dolomite.....	55
<b>Fig. 4.5.</b> Eh-pH predominance diagram of As at 25°C, 1.013 bar, activity of As = 10 <sup>-6</sup> , activity of SO <sub>4</sub> <sup>2-</sup> = 10 <sup>-3</sup> and activity of Ca <sup>2+</sup> = 10 <sup>-3</sup> . The diagram was created using the Geochemist's Workbench®. ....	56
<b>Fig. 4.6.</b> Leaching concentration of Mg <sup>2+</sup> versus the amount of half-burnt dolomite addition.....	57
<b>Fig. 4.7.</b> Effects of addition of half-burnt dolomite on As leaching .....	58
<b>Fig. 4.8.</b> Effects of addition of iron oxide on As leaching .....	59
<b>Fig. 4.9.</b> Leaching concentration of Ca <sup>2+</sup> versus the amount of iron oxide addition .....	60
<b>Fig. 4.10.</b> Leaching concentration of SO <sub>4</sub> <sup>2-</sup> versus the amount of iron oxide addition ..	61
<b>Fig. 4.11.</b> The molar ratio of Ca <sup>2+</sup> to SO <sub>4</sub> <sup>2-</sup> versus the amount of iron oxide addition ..	61
<b>Fig. 4.12.</b> Schematic diagram of As adsorption/precipitation on iron oxide.....	62
<b>Fig. 4.13.</b> Leaching concentration of As versus concentrations of HCO <sub>3</sub> <sup>-</sup> and CO <sub>3</sub> <sup>2-</sup> in case of iron oxide addition.....	63
<b>Fig. 4.14.</b> The changes in ATR-FTIR of soil sample A with and without adsorbents...	67
<b>Fig. 4.15.</b> Effects of foam reagent and coagulant on As leaching.....	68

## LIST OF TABLES

<b>Table 3.1.</b> Mineralogical properties and the types of soil samples tested.....	22
<b>Table 3.2.</b> Chemical compositions of soil samples tested .....	23
<b>Table 4.1.</b> Chemical compositions of magnesium oxide (denite™), half-burnt dolomite, and iron oxide .....	46
<b>Table 4.2.</b> Details of cases of batch leaching experiments .....	47
<b>Table 4.3.</b> Saturation indices of possible Mg-minerals in leachate of batch leaching experiments with magnesium oxide addition .....	54
<b>Table 4.4.</b> Results of the principal component analysis in case of magnesium oxide addition .....	64
<b>Table 4.5.</b> Results of the principal component analysis in case of half-burnt dolomite addition .....	65
<b>Table 4.6.</b> Results of the principal component analysis in case of iron oxide addition. ....	65

# CHAPTER 1

## GENERAL INTRODUCTION

### 1.1 Arsenic contamination in soils

Arsenic (As) is a well-known toxic element and prolonged exposure to As even in a minute concentration causes a number of serious diseases (Chakraborty et al., 2017; Fayiga and Saha, 2016, Lü et al., 2018, Suda and Makino, 2016). According to Grosz et al. (2004), Sultan (2007), and Zhang et al. (2006), the distributions of As in soils are mostly controlled by the bedrock characteristics. The average As content in the Earth's crust is about 1 mg/kg (Drahota and Filippi, 2009) while Wang and Mulligan (2006) reported that the naturally occurring As contents in soil in Canada range from 4.8 to 13.6 mg/kg. Meanwhile, As distribution in Hokkaido, Japan is shown in the Fig. 1.1, which is divided into 8 classifications ranging from 0.00863 to 856 mg/kg.

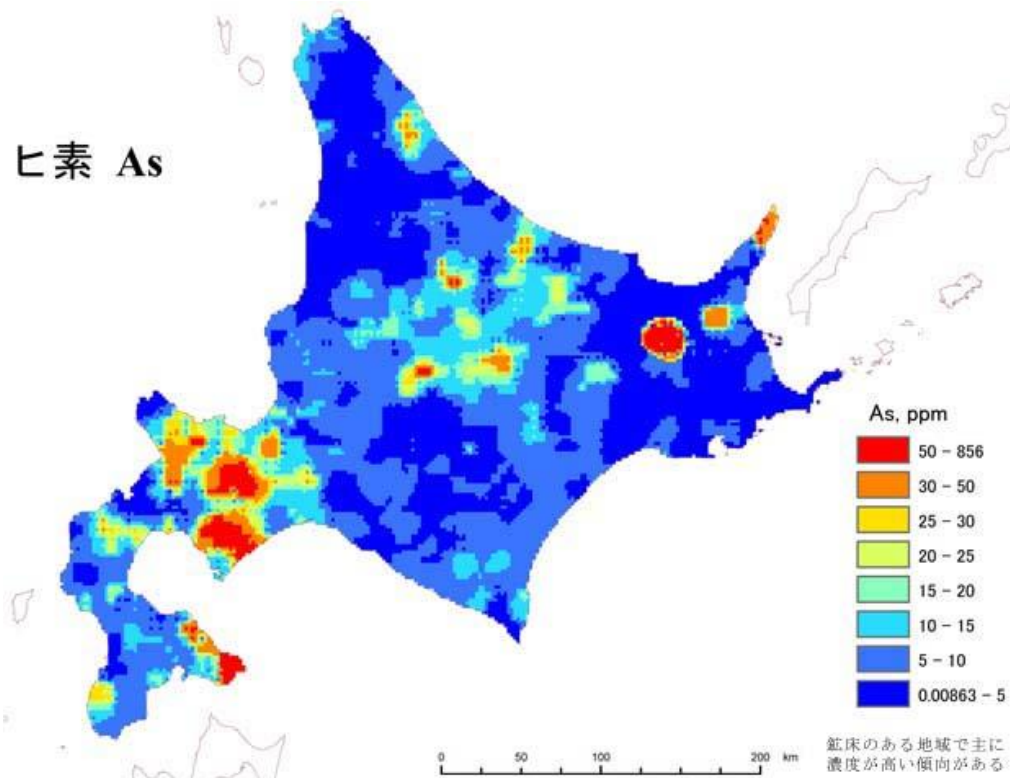


**Fig. 1.1.** Arsenic distribution in Hokkaido

(<https://gbank.gsj.jp/geochemmap/Hokkaido/gazou/hokkaidoAs-s.jpg>)

## 1.2 Geochemistry of arsenic in environments

A generalized geochemical cycle of As is shown in Figure 1.2. In nature, As can exist in the biosphere, atmosphere, hydrosphere, pedosphere, and the lithosphere with any one of four different oxidation states: As(-III), As(0)-metallic arsenic, As(III) and As(V). Both As(III) and As(V) can be found as inorganic and organic metallic species (Boyle and Jonasson, 1973; Ferguson and Gavis, 1972; Wang and Mulligan, 2005). Arsenic in the biosphere is probably that all plants and animals contain As while As in the atmosphere is mainly due to human's activity, which is attributed to the burning and smelting processes. Arsenic contained in natural water such as hot springs, stream, river, lake, ocean, and ground water contributes to As in the hydrosphere. Groundwater may be enriched in As when they locate near arseniferous deposits whereas hot springs in active volcanic terranes carry high amounts of As. Arsenic in the pedosphere mainly depends on the properties of original rocks formed compared with anthropogenic activities. Meanwhile, As in the lithosphere is the result of As-bearing minerals contained in the igneous, sedimentary, and metamorphic rocks. Among As-bearing minerals, pyrite contains a huge amount of As (Boyle and Jonasson, 1973).

The Eh-pH diagram for aqueous As species is shown in Fig. 1.3 (Smedley and Kinniburgh, 2002). Arsenite (As(III)) is the dominant form under reducing conditions whereas well-oxygenated environments is a thermodynamically favorable conditions for arsenate (As(V)) form. Meanwhile, arsenite can be found as  $\text{H}_3\text{AsO}_3$ ,  $\text{H}_2\text{AsO}_3^-$ ,  $\text{HAsO}_3^{2-}$ , or  $\text{AsO}_3^{3-}$  forms depending on pH while those of arsenate are  $\text{H}_3\text{AsO}_4$ ,  $\text{H}_2\text{AsO}_4^-$ ,  $\text{HAsO}_4^{2-}$ , and  $\text{AsO}_4^{3-}$  forms.

## 1.3 The removal of arsenic

The removal of inorganic As from water in industrial scales or smaller scale water treatment facilities can be done by many treatment technologies. Conventional coagulation, filtration process, or lime softening process is considered as practical methods to remove As. Among these methods, adding adsorbents is one of the convenient methods. Irrespective of a variety of adsorbents used such as iron-oxide-coated diatomite, iron-oxide-coated cement, granular ferric hydroxide, iron oxide permeated mesoporous rice-husk nanobiochar, iron-rich industrial by-products, iron-based amendments, pedogenic Fe-Mn nodule material, ferrihydrite, steelmaking slag

and limestone, untreated dolomite powder, iron oxide-coated sand, natural iron oxide mineral, lignite, bentonite, shale, and iron sand, magnesium oxide (MgO) and half-burnt dolomite (MgO.CaCO<sub>3</sub>) are reported as the effective adsorbents in the alkaline pH region (Tresintsi et al., 2014) whereas iron oxide adsorbent (Fe<sub>2</sub>O<sub>3</sub>) is often used for As(V) adsorption. Moreover, they are considered as economical and easily available adsorbents.

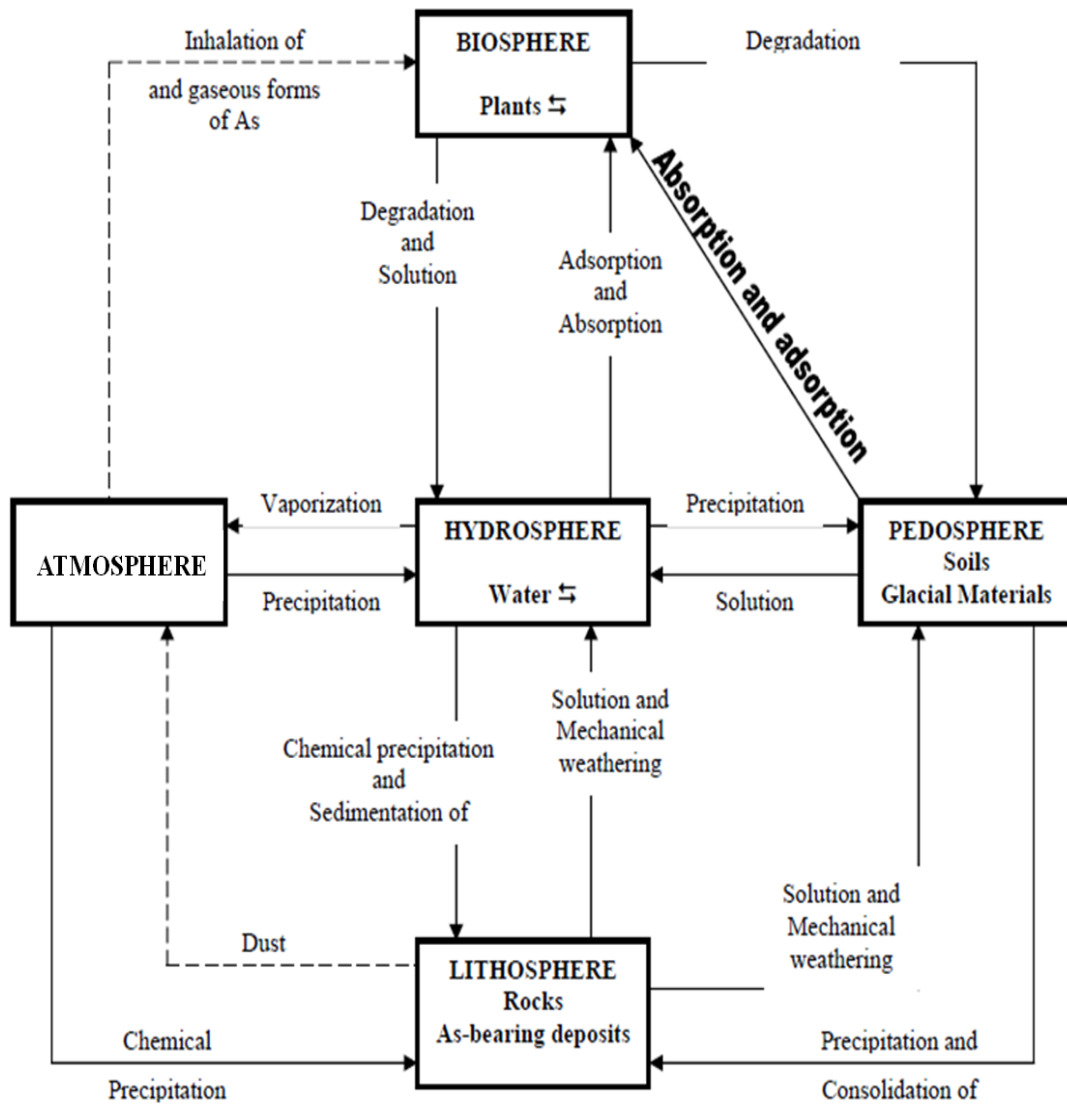


**Fig. 1.2.** Generalized geochemical cycle of arsenic (Boyle and Jonasson, 1973)

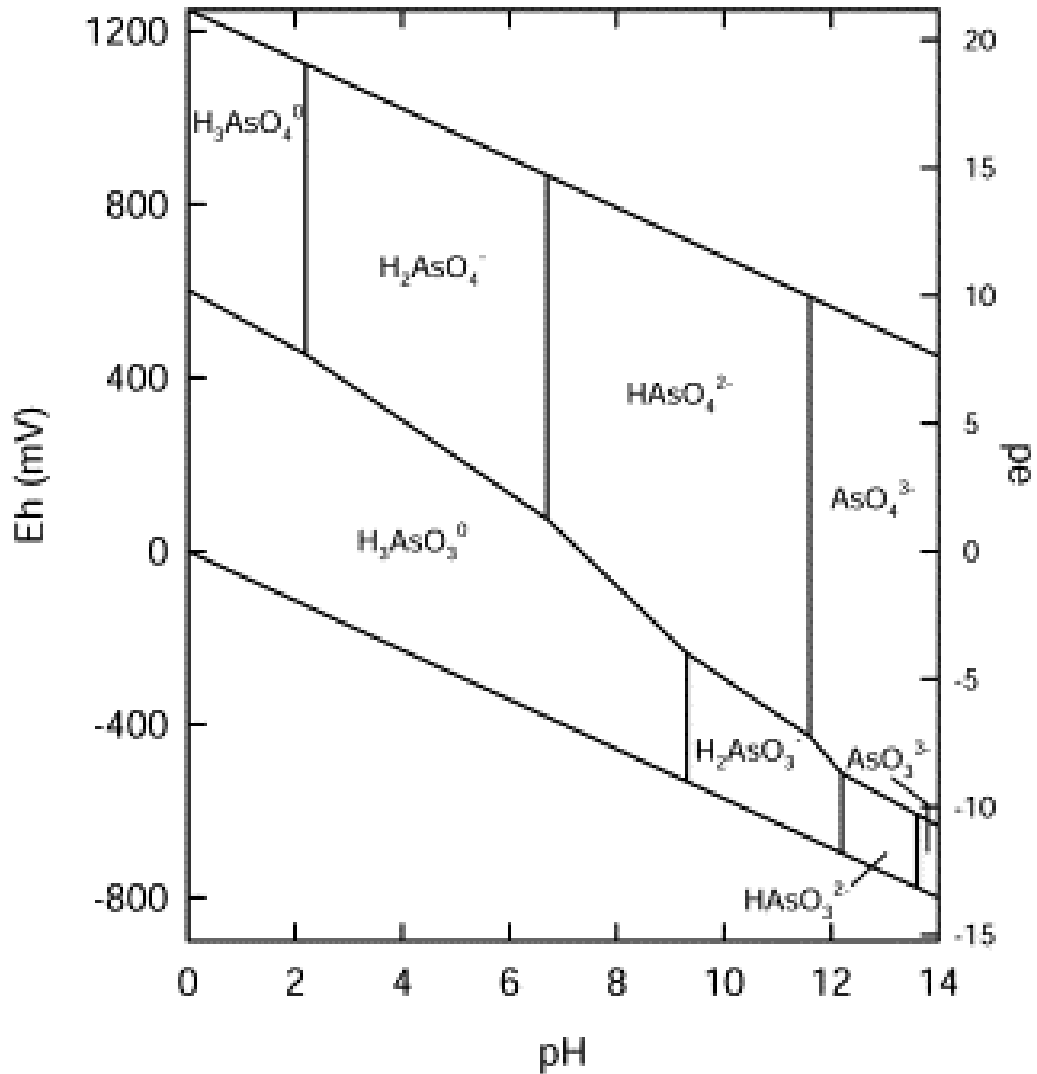


**Fig. 1.3.** Eh-pH diagram of As species for an As-O<sub>2</sub>-H<sub>2</sub>O system at 25°C and 1 bar  
(Smedley and Kinniburgh, 2002)

#### 1.4 Shield-tunneling excavation

Origin of shield tunneling was developed as a method of digging tunnels through the soft ground. The basic concept of shield-tunneling is to press a rigid shield forward through soft ground with jacks, thus preventing the ground from collapsing, and build the tunnel structure within the frames. Shield-tunneling is a technique originally developed in England (Konda, 2001) while it is suited to conditions in Japan, where space is short, soft alluvial deposits are widespread, and the demand for tunnels is high (Konda, 2001).

## References

- AIST (National Institute of Advanced Industrial Science and Technology), (2021). Geological survey, <https://gbank.gsj.jp/geochemmap/Hokkaido/gazou/hokkaidoAs-s.jpg>, last visited January 2021.
- Boyle, R. W., Jonasson, I. R., 1973. The geochemistry of arsenic and its use as an indicator element in geochemical prospecting. *Journal of Geochemical Exploration*, 2(3), 251-296.
- Chakraborty, S., Li, B., Deb, S., Paul, S., Weindorf, D. C., Das, B. S., 2017. Predicting soil arsenic pools by visible near infrared diffuse reflectance spectroscopy. *Geoderma*, 296, 30-37.
- Drahota, P., Filippi, M., 2009. Secondary arsenic minerals in the environment: a review. *Environment International*, 35(8), 1243-1255.
- Fayiga, A. O., Saha, U. K., 2016. Arsenic hyperaccumulating fern: implications for remediation of arsenic contaminated soils. *Geoderma*, 284, 132-143.
- Ferguson, J. F., Gavis, J., 1972. A review of the arsenic cycle in natural waters. *Water Research*, 6(11), 1259-1274.
- Grosz, A. E., Grossman, J. N., Garrett, R., Friske, P., Smith, D. B., Darnley, A. G., Vowinkel, E., 2004. A preliminary geochemical map for arsenic in surficial materials of Canada and the United States. *Applied Geochemistry*, 19(2), 257-260.
- Konda, T., 2001. Shield tunneling method. *Civil Engineering*, Japan Society of Civil Engineering, 39, 23-27.
- Lü, J., Jiao, W. B., Qiu, H. Y., Chen, B., Huang, X. X., Kang, B., 2018. Origin and spatial distribution of heavy metals and carcinogenic risk assessment in mining areas at You'xi County southeast China. *Geoderma*, 310, 99-106.
- Smedley, P. L., Kinniburgh, D. G., 2002. A review of the source, behavior and distribution of arsenic in natural waters. *Applied Geochemistry*, 17, 517-568.
- Suda, A., Makino, T., 2016. Functional effects of manganese and iron oxides on the dynamics of trace elements in soils with a special focus on arsenic and cadmium: a review. *Geoderma*, 270, 68-75.
- Sultan, K., 2007. Distribution of metals and arsenic in soils of Central Victoria (Creswick-Ballarat), Australia. *Archives of Environmental Contamination and Toxicology*, 52(3), 339-346.

- Tresintsi, S., Simeonidis, K., Katsikini, M., Paloura, E. C., Bantsis, G., Mitrakas, M., 2014. A novel approach for arsenic adsorbents regeneration using MgO. *Journal of Hazardous Materials*, 265, 217-225.
- Wang, S., Mulligan, C. N., 2006. Occurrence of arsenic contamination in Canada: sources, behavior and distribution. *Sci. Total Environ.*, 366(2-3), 701-721.
- Zhang, H. H., Yuan, H. X., Hu, Y. G., Wu, Z. F., Zhu, L. A., Zhu, L., Li, D. Q., 2006. Spatial distribution and vertical variation of arsenic in Guangdong soil profiles, China. *Environmental Pollution*, 144(2), 492-499.



## CHAPTER 2

### LITERATURE REVIEW

#### 2.1 The recent studies regarding the As leaching characteristics

Arsenic (As) leaching characteristics from rocks excavated from underground tunnel projects have been studied by many researchers. Igarashi et al. (2008), Tabelin and Igarashi (2009), and Tabelin et al. (2014a, b), for example, highlighted the importance of pH and redox potential (Eh) in the speciation and mobility of As from sedimentary and volcanic rocks. In more details, As leaching as a function of pH from hydrothermally altered igneous rocks is shown in Fig. 2.1 (Tabelin and Igarashi, 2009). In the oxic conditions, the shape of As mobilization depends on pH like “V”-shaped graph with the minimum leaching concentrations observed at neutral pH whereas leaching concentrations of As were enhanced in both acidic and alkaline pH regions. Similar behaviors of As leaching from sedimentary rocks, which strongly depends on pH (Fig. 2.2), were also observed by Tabelin et al., (2014a). Leaching concentrations of As were lower in circumtance pH while those in the acidic or alkaline pH regions were higher. This may be mainly because of the nature of As.

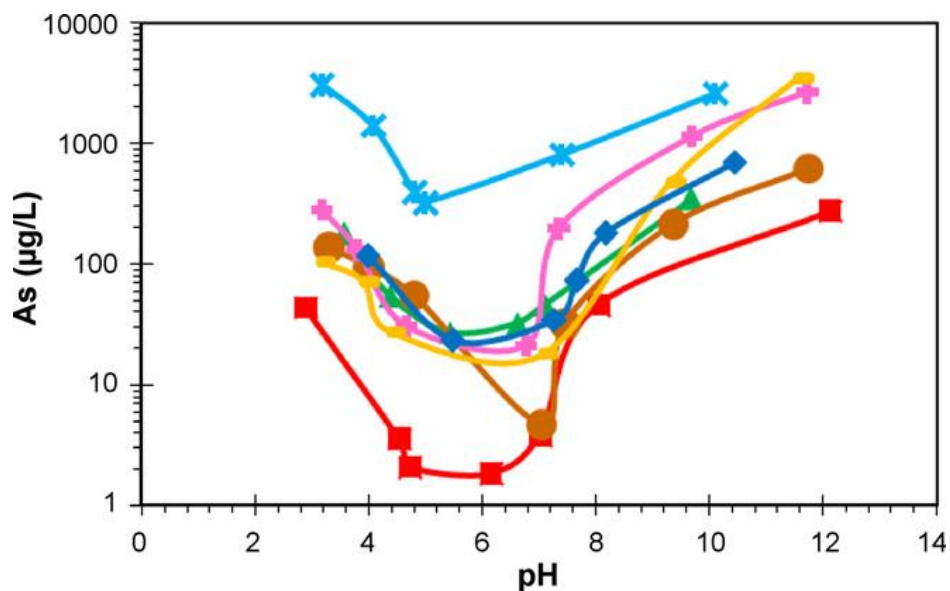


**Fig. 2.1.** As leaching concentration from hydrothermally altered igneous rocks as a function of pH under oxic conditions (Tabelin and Igarashi, 2009)

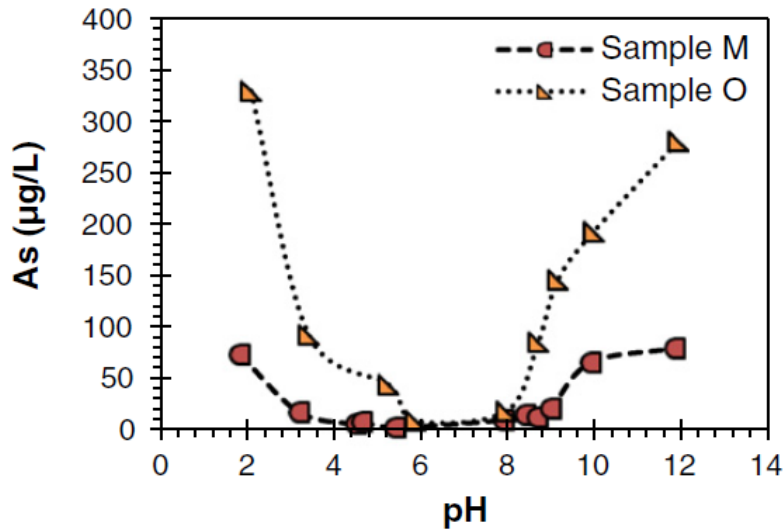


**Fig. 2.2.** Leaching behaviors of As from sedimentary rocks as a function of pH (Tabelin et al., 2014a)

There are also published works about the leaching characteristics of As from contaminated soils and industrial wastes such as stabilization/solidification treated soils (Li et al., 2017; Moon et al., 2008; Yoon et al., 2010), agricultural soils (Casentini et al., 2011; Chiang et al., 2010; Dousova et al., 2016), contaminated landfill soils (Azhar et al., 2016; Delemos et al., 2006; Ghosh et al., 2004, 2006), volcanic soils (Tatsuhara et al., 2012), fly ash (Marove et al., 2020), floodplain soils (Frohne et al., 2011; Yun et al., 2016), contaminated acid soils (Aguilar-Carrillo et al., 2009), mine-affected contaminated soils (Lee, 2006 ; Manzano et al., 2016; Neel et al., 2003; Pérez-de-Mora et al., 2007; Silvetti et al., 2014), and mine tailings (Kalinowski et al., 2004).

In addition, Gersztyn et al. (2013) studied on the impact of pH adjusted by various doses of hydrochloric acid (HCl) and sodium hydroxide (NaOH) on the solubility of As in heavily contaminated soils. In order to achieve the purpose of the study, three soil samples collected from the former As industry area with the differences in initial pH, calcium carbonate, organic matter, and total As contents were tested. The results indicated that As solubility in the contaminated soils was low at neutral or slightly acidic pH and increased considerably when the pH leachate became more acidic or more alkaline as shown in Fig. 2.3. These results were well consistent with the results of behaviors of As leaching from the sedimentary rocks and hydrothermally altered igneous rocks as reviewed above.

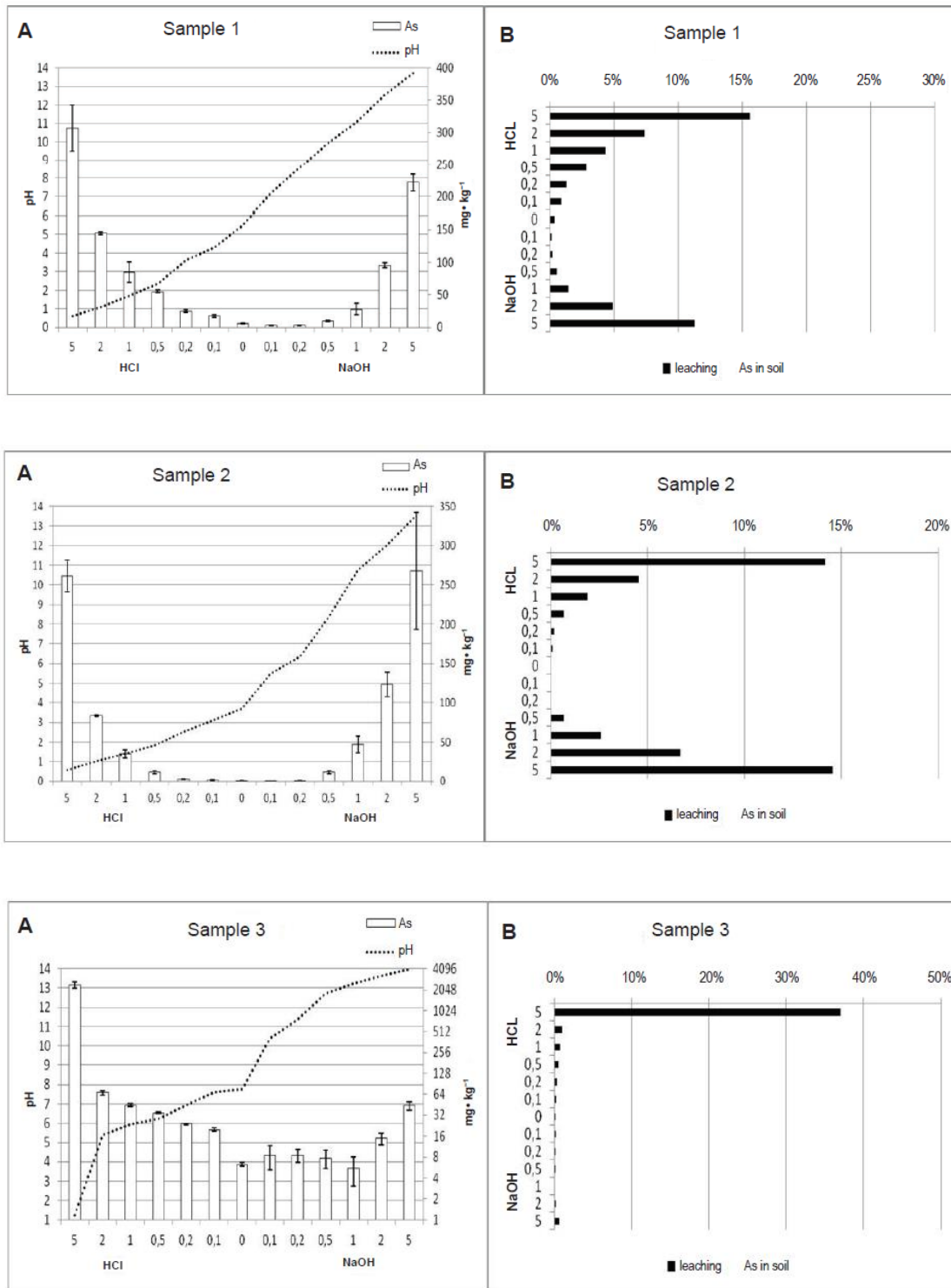


**Fig. 2.3.** Changes in pH and arsenic solubility in samples 1, 2 and 3, as affected by various doses of HCl and NaOH. Doses are expressed in cm<sup>3</sup> of 1 mol/dm<sup>3</sup> HCl or 1 mol/dm<sup>3</sup> NaOH per 5 g soil. Arsenic release is illustrated in mg/kg (A) and as a percentage of the total arsenic in soils (B) (Gersztyn et al., 2013).

## **2.2 Statement of the problem and objectives of the study**

A massive volume of soils excavated by shield-tunneling excavation are produced. Improper managements of the excavated soils causes As leaching. This is because changes in pH due to cement addition mobile natural occurring As from these alkaline excavated soils. In spite of the fact that a number of researches have been conducted on the effects of pH on As leaching, those researches just focus on the effects of pH on As leaching from the materials other than shield-tunneling excavated soils or As leaching from rocks/soils as a function of pH by changing the pH with HCl and NaOH. Therefore, the main objective of the present study is to evaluate the effects of pH on As leaching from shield-tunneling excavated soil by cement addition, and As leaching countermeasure is then investigated. The detail objectives can be listed as follow:

- a. To evaluate leaching concentration of As from the soil samples involved in shield-tunneling excavation
- b. To evaluate the effects of cement addition on As leaching from the excavated soils
- c. To evaluate the performances of magnesium oxide, half-burnt dolomite, and iron oxide absorbents on As leaching from the excavated soils, and
- d. To evaluate the effects of commonly used foam reagent and coagulant on As leaching from the excavated soils

## **2.3 Outline of dissertation**

This dissertation consists of five chapters and the outline is as follow:

In chapter 1, As contamination in soils, geochemistry of As in environments, the removal of As, and shield-tunneling excavation are briefly reviewed and introduced.

There have been a number of publications on the characteristics of As leaching from soils, rocks, or industrial wastes. However, these studies focused on soils, rocks, or materials other than shield-tunneling excavated soils. In other words, the effects of pH on As leaching from shield-tunneling excavated soils is not well understood. Therefore, chapter 2—literature review chapter—will be a brief summary of the recent studies

regarding the As leaching characteristics, and the necessities and objectives of the present study are then depicted in this chapter.

When the important underground-facilities need to be constructed under soft ground, shield-tunneling excavated method is utilized. It is because this technique could improve the stabilization of the ground. In this excavation method, cement is always used for reinforcing the excavated tunnel walls. Although cement addition could improve the mechanical properties of soft soils and sediments, this process inadvertently increases soil pH, resulted in mobilizing naturally occurring As as mentioned in literature review of the above chapter. However, how the excavated soils can be affected by cement addition is still not well understood. Therefore, chapter 3 is conducted to elucidate the effects of cement addition on As leaching from soils excavated by the shield-tunneling method.

After identifying the effects of cement addition on As leaching, the countermeasure of As leaching is carefully considered. The performance of magnesium oxide, half-burnt dolomite, and iron oxide absorbents on As leaching from the soils are evaluated and compared. In addition to cement, which is always needed for reinforcing the excavated tunnel walls, commonly used foam reagent and coagulant are also used in cases needed for enhancing the excavation performance. Thus, the effects of the foam reagent and coagulant are also evaluated in chapter 4.

Finally, chapter 5 summarizes all general conclusions of the present study.

## References

- Aguilar-Carrillo, J., Garrido, F., Barrios, L., García-González, M. T., 2009. Induced reduction of the potential leachability of As, Cd and Tl in an element-spiked acid soil by the application of industrial by-products. *Geoderma*, 149(3-4), 367-372.
- Azhar, A. T. S., Azim, M. A. M., Aziman, M., Nabila, A. T. A., 2016. Leachability of arsenic (As) contaminated landfill soil stabilised by cement and bagasse ash. In *IOP Conference Series: Materials Science and Engineering* (Vol. 160, No. 1, 012078). IOP Publishing.
- Casentini, B., Hug, S. J., Nikolaidis, N. P., 2011. Arsenic accumulation in irrigated agricultural soils in Northern Greece. *Sci. Total Environ.*, 409(22), 4802-4810.
- Chiang, K. Y., Lin, K. C., Lin, S. C., Chang, T. K., Wang, M. K., 2010. Arsenic and lead (beudantite) contamination of agricultural rice soils in the Guandu Plain of northern Taiwan. *Journal of Hazardous Materials*, 181(1-3), 1066-1071.
- Delemos, J. L., Bostick, B. C., Renshaw, C. E., Stürup, S., Feng, X., 2006. Landfill-stimulated iron reduction and arsenic release at the Coakley Superfund Site (NH). *Environmental Science & Technology*, 40(1), 67-73.
- Dousova, B., Buzek, F., Lhotka, M., Krejcová, S., Boubinová, R., 2016. Leaching effect on arsenic mobility in agricultural soils. *Journal of Hazardous Materials*, 307, 231-239.
- Frohne, T., Rinklebe, J., Diaz-Bone, R. A., Du Laing, G., 2011. Controlled variation of redox conditions in a floodplain soil: Impact on metal mobilization and biomethylation of arsenic and antimony. *Geoderma*, 160(3-4), 414-424.
- Gersztyn, L., Karczewska, A., Gałka, B., 2013. Influence of pH on the solubility of arsenic in heavily contaminated soils. *Environmental Protection and Natural Resources*, 24(3), 7-11.
- Ghosh, A., Mukiibi, M., Ela, W., 2004. TCLP underestimates leaching of arsenic from solid residuals under landfill conditions. *Environmental Science & Technology*, 38(17), 4677-4682.

- Ghosh, A., Mukiibi, M., Sáez, A. E., Ela, W. P., 2006. Leaching of arsenic from granular ferric hydroxide residuals under mature landfill conditions. *Environmental Science & Technology*, 40(19), 6070-6075.
- Igarashi, T., Imagawa, H., Uchiyama, H., Asakura, K., 2008. Leaching behavior of arsenic from various rocks by controlling geochemical conditions. *Miner. Eng.*, 21, 191-199.
- Kalinowski, B. E., Oskarsson, A., Albinsson, Y., Arlinger, J., Ödegaard-Jensen, A., Andlid, T., Pedersen, K., 2004. Microbial leaching of uranium and other trace elements from shale mine tailings at Ranstad. *Geoderma*, 122(2-4), 177-194.
- Lee, S., 2006. Geochemistry and partitioning of trace metals in paddy soils affected by metal mine tailings in Korea. *Geoderma*, 135, 26-37.
- Li, J. S., Beiyuan, J., Tsang, D. C. W., Wang, L., Poon, C. S., Li, X. D., Fendorf, S., 2017. Arsenic-containing soil from geogenic source in Hong Kong: Leaching characteristics and stabilization/solidification. *Chemosphere*, 182, 31-39.
- Manzano, R., Silveti, M., Garau, G., Deiana, S., Castaldi, P., 2016. Influence of iron-rich water treatment residues and compost on the mobility of metal(loid)s in mine soils. *Geoderma*, 283, 1-9.
- Marove, C. A., Tangviroon, P., Tabelin, C. B. and Igarashi, T., 2020. Leaching of hazardous elements from Mozambican coal and coal ash. *Journal of African Earth Sciences* 168, 103861.
- Moon, D. H., Wazne, M., Yoon, I. H., Grubb, D. G., 2008. Assessment of cement kiln dust (CKD) for stabilization/solidification (S/S) of arsenic contaminated soils. *Journal of Hazardous Materials*, 159(2-3), 512-518.
- Neel, C., Bril, H., Courtin-Nomade, A., Dutreuil, J. P., 2003. Factors affecting natural development of soil on 35-year-old sulphide-rich mine tailings. *Geoderma*, 111(1-2), 1-20.

- Pérez-de-Mora, A., Madrid, F., Cabrera, F., Madejón, E., 2007. Amendments and plant cover influence on trace element pools in a contaminated soil. *Geoderma*, 139(1-2), 1-10.
- Silvetti, M., Castaldi, P., Holm, P. E., Deiana, S., Lombi, E., 2014. Leachability, bioaccessibility and plant availability of trace elements in contaminated soils treated with industrial by-products and subjected to oxidative/reductive conditions. *Geoderma*, 214, 204-212.
- Tabelin, C. B., Igarashi, T., 2009. Mechanisms of arsenic and lead release from hydrothermally altered rock. *Journal of Hazardous Materials*, 169(1-3), 980-990.
- Tabelin, C. B., Hashimoto, A., Igarashi, T., Yoneda, T., 2014a. Leaching of boron, arsenic and selenium from sedimentary rocks: I. Effects of contact time, mixing speed and liquid-to-solid ratio. *Sci. Total Environ.*, 472, 620–629.
- Tabelin, C. B., Hashimoto, A., Igarashi, T., Yoneda, T., 2014b. Leaching of boron, arsenic and selenium from sedimentary rocks: II. pH dependence, speciation and mechanisms of release. *Sci. Total Environ.*, 473, 244-253.
- Tatsuhara, T., Arima, T., Igarashi, T., Tabelin, C. B., 2012. Combined neutralization–adsorption system for the disposal of hydrothermally altered excavated rock producing acidic leachate with hazardous elements. *Eng. Geol.*, 139, 76–84.
- Yoon, I. H., Moon, D. H., Kim, K. W., Lee, K. Y., Lee, J. H., Kim, M. G., 2010. Mechanism for the stabilization/solidification of arsenic-contaminated soils with Portland cement and cement kiln dust. *Journal of Environmental Management*, 91(11), 2322-2328.
- Yun, S. W., Park, C. G., Jeon, J. H., Darnault, C. J., Baveye, P. C., Yu, C., 2016. Dissolution behavior of As and Cd in submerged paddy soil after treatment with stabilizing agents. *Geoderma*, 270, 10-20.



## CHAPTER 3

# EFFECTS OF CEMENT ADDITION ON ARSENIC LEACHING FROM SOILS EXCAVATED FROM PROJECTS EMPLOYING SHIELD-TUNNELING METHOD

### 3.1 Introduction

Due to rapid population growth and urbanization, utilization of underground space has become more widespread in recent years. For example, numerous tunnels have been constructed in Japan, China and the European Union for various purposes like railway and highway network expansions, new bullet/high speed train routes, hydro-electric powerplants, shopping malls, parking spaces and sewer/utility systems (Tabelin et al., 2018). Among the various tunnel excavation methods, shield-tunneling—a technique originally developed in England (Konda, 2001) for mechanically weak geological lithologies—was first adopted in Nagoya city, Japan for a subway project (Koyama, 2003). The shield-tunneling method controls ground movements (Koyama, 2003), so it could enhance stabilization of both the ground and tunnel surfaces. In order to achieve this, however, cementitious materials are required to improve the mechanical strength of weak geological lithologies, a practice that inadvertently increases the soil pH because cement is inherently alkaline (Ghazvini et al., 2009).

Arsenic (As) is a well-known toxic element and is often found in natural soils, sediments and rocks in minute amounts (<10 mg/kg) (Huyen et al., 2019a, b; Tabelin et al., 2012a; Tamoto et al., 2015). Under certain geochemical conditions, however, the leaching concentration of As from soils could exceed the World Health Organization (WHO) provisional drinking water standard of 10 µg/L (Tabelin et al., 2014a). Prolonged exposure to As even in minute concentrations could increase the risks of developing cancers of the skin, kidney and bladder (Farzan et al., 2013; O'Day et al., 2004; Rahman et al., 2009; Smedley and Kinniburgh, 2002; Tchounwou et al., 2004).

Many researchers have studied As leaching characteristics from soils or rocks excavated from underground tunnel projects. Igarashi et al. (2008), Tabelin and Igarashi (2009), and Tabelin et al. (2014b, c), for example, highlighted the importance of pH and

redox potential (Eh) in the speciation and mobility of As from sedimentary and volcanic rocks. There are also published works about the leaching characteristics of As from contaminated soils and industrial wastes such as stabilization/solidification treated soils (Li et al., 2017; Moon et al., 2008; Yoon et al., 2010), agricultural soils (Casentini et al., 2011; Chiang et al., 2010; Dousova et al., 2016), contaminated landfill soils (Azhar et al., 2016; Delemos et al., 2006; Ghosh et al., 2004, 2006), volcanic soils (Tatsuhara et al., 2012), fly ash (Marove et al., 2020), floodplain soils (Frohne et al., 2011; Yun et al., 2016), contaminated acid soils (Aguilar-Carrillo et al., 2009), mine-affected contaminated soils (Lee, 2006; Manzano et al., 2016; Neel et al., 2003; Pérez-de-Mora et al., 2007; Silvetti et al., 2014), mine tailings (Kalinowski et al., 2004) and heavily As-contaminated soils (Gersztyn et al., 2013). However, these studies focused on either rocks, soils or materials other than shield-tunneling excavated soils, or the characteristics of As leaching from rocks/soils versus pH by changing the pH with hydrochloric acid (HCl) and sodium hydroxide (NaOH). In other words, leaching of naturally occurring As from soils related to pH change by cement addition during shield-tunneling is still not well understood. Therefore, the present study was carried out to elucidate the effects of cement addition on As leaching from soils and determine the mechanisms controlling the release of As from excavated soils by shield-tunneling.

## **3.2 Materials and Methods**

### ***3.2.1 Characterization of soil samples***

The soil samples used in the present study were obtained from borehole cores collected for a tunnel construction project in Sapporo city, Hokkaido, Japan. Soft alluvial deposits, which belong to the Quaternary with geological ages from the late Pleistocene to Holocene, dominate the geology of Sapporo. Naturally occurring As in the geological layers was likely transported by the Toyohira River from upstream sources like marine sedimentary rocks as it forms an alluvial fan (Tatsumi et al., 2006). Eight soil samples were collected from three different boreholes by considering the texture. The type and sampling depth are shown in Table 3.1. Samples A, B, C, D, and E were taken from borehole B1 at different depths. Sample F was collected from a different borehole (B2). Meanwhile, Samples G and H were sampled at different depths of another borehole (B3). In the laboratory, the soil samples were air dried, manually

crushed using an agate mortar and pestle and sieved to less than 2 mm in diameter for leaching and sequential extraction experiments.

To determine the chemical and mineralogical compositions, the samples were further crushed to finer than 50  $\mu\text{m}$  and then analyzed by X-ray fluorescence spectroscopy (XRF) (SpectroXepos, Rigaku Corporation, Japan) and X-ray powder diffraction (XRD) (MultiFlex, Rigaku Corporation, Japan). All XRD patterns of the original soils and soils with cement after the batch leaching experiments were analyzed using Match!® software (Crystal Impact, Germany). These samples were also analyzed by attenuated total reflectance Fourier transform infrared spectroscopy (ATR-FTIR) (FT/IR-6200 HFV and ATR Pro One attachment equipped with a diamond prism, Jasco Analytical Instruments, Japan). Finally, the zeta potential distribution of soil samples with pH was measured using Nano-ZS60 (Malvern Instruments, UK).

A total carbon analyzer with solid sample combustion unit (TOC-VCSH-SSM-5000A, Shimadzu Corporation, Japan) was used to quantify both total carbon (TC) and inorganic carbon (IC) of soil samples, and the total organic carbon (TOC) was calculated based on the difference between TC and IC. Total As content in the soil was evaluated by the result of sequential extraction. In addition, soil types were determined by standard sieving and laser diffraction (Microtrac® MT3300SX, Nikkiso Co., Ltd., Japan).

### ***3.2.2 Batch leaching experiments***

Batch leaching experiments were conducted to evaluate the change in leaching concentrations of As from soils by assuming that the shield-tunneling technique was adopted. Thus, batch leaching experiments with and without cement were conducted to understand the effects of cement addition on As leaching. In the present study, commercial ordinary Portland cement (OPC), which contains CaO as the main component, was used. The OPC consists of around 63% of CaO, 21% of SiO<sub>2</sub>, 5% of Al<sub>2</sub>O<sub>3</sub>, 5% of Fe<sub>2</sub>O<sub>3</sub>, followed by a few percentages of minor oxides such as SO<sub>3</sub>, MgO, K<sub>2</sub>O, Na<sub>2</sub>O. This type of cement was selected because of its low-cost, availability, and widespread use (Ojovan, 2011). In addition, the shield-tunneling machine moves relatively quickly when it is working. This means that the shield-tunneling excavation method needs a type of cement that enables the wall of excavated tunnel to harden

quickly. Meanwhile, the OPC has high initial setting time. Moreover, high, long-term durability imparted by special cement like blast-furnace slag cement (Ojovan, 2011) is not required. Two types of experiments were conducted: (i) leaching without cement, and (ii) leaching with cement. In the batch leaching experiments without cement, 15 g of soil sample were mixed with 150 ml of deionized (DI) water in a 300-ml Erlenmeyer flask. The mixture was shaken at 120 rpm for 24 hours under ambient conditions. After the predetermined shaking time, the suspension was collected for pH, electrical conductivity (EC), and oxidation-reduction potential (ORP) measurements. The leachate was then collected by filtering the suspension using 0.45  $\mu\text{m}$  Millex® membrane filters (Merck Millipore, USA). The leaching experiments were conducted in triplicates to ensure that variations and trends observed in the data are statistically significant.

For the alkalinity measurements, a known volume of leachate sample was titrated with 0.01M sulfuric acid ( $\text{H}_2\text{SO}_4$ ) until pH 4.8. Meanwhile, concentrations of major ions in the leachate were determined by inductively coupled plasma atomic emission spectroscopy (ICP-AES) (ICPE-9000, Shimadzu Corporation, Japan) (margin of error =  $\pm 2\%$ ) while concentrations of As were quantified by ICP-AES with a hydride-vapor generator (HVG) attachment (detection limit = 0.1  $\mu\text{g/L}$ ; margin of error =  $\pm 5\%$ ). Prior to the measurement of As concentration by ICP-AES-HVG, the leachate samples were pretreated as follows: 10 ml of leachate samples were mixed with 5 ml of 12 M hydrochloric acid (HCl), 0.33 ml of ascorbic acid, 0.67 ml of 20% potassium iodide (KI), and 0.67 ml of DI water. In the batch leaching experiments with cement, the procedure was the same as the batch leaching experiments without cement. For Samples A, D, and F, the mixture of soil and cement was added to a 300-ml Erlenmeyer flask with 150 ml of DI water. The cement addition to soils were 0.2, 0.3, 0.5, 1, and 2% by weight for Sample A; 0.2, 0.3, 0.5, 1, 1.5, and 2% by weight for Sample D; and 0.1, 0.2, 0.3, 0.5, 1, 2, 3, and 4% by weight for Sample F. The cement percentages were determined by considering the ratio between cement and soils. For example, the cement addition percentage to soil of 0.2% means that 15 g of soil sample was mixed with 0.03 g of cement. These cases were selected to cover a wide pH range in the experiments.

The residue in the flask was analyzed by XRD, XRF and ATR-FTIR after drying at room temperature. The XRD and XRF analyses were conducted to identify the

minerals produced and the change in chemical compositions due to cement addition, respectively, whereas the ATR-FTIR analysis was conducted to evaluate changes in molecular bonding and coordination of As in the soil samples.

The chemical species of As was modeled using the Geochemist's Workbench® (Bethke and Yeakel, 2011) based on the concentrations of As and major ions measured in the leaching experiments.

### ***3.2.3 Sequential extraction***

The sequential extraction procedure used in the present study was developed by Marumo et al. (2003) based on the earlier work of Tessier et al. (1979). This method is one of the most common methods for contaminated soil and sediment samples (Abollino et al., 2006; Gleyzes et al., 2002; Silwamba et al., 2020). One gram of soil sample was mixed with an extractant in a centrifuge tube. Arsenic fraction of the soil sample can be divided into five. The details of the volume of extractants, temperature, pH, mixing speed, and extraction time are listed as follows:

- Step 1 (Exchangeable): One gram of soil sample was mixed with 20 ml of 1M NaH<sub>2</sub>PO<sub>4</sub> at pH 5. The mixture was shaken at 200 rpm for 1 hour at room temperature.
- Step 2 (Bound to carbonates): The residual soil sample from step 1 was extracted with 20 ml of 1M CH<sub>3</sub>COONa of pH 5 at 200 rpm for 5 hours at room temperature.
- Step 3 (Bound to iron and manganese oxides): The residual soil sample from step 2 was mixed with 20 ml of 0.04M NH<sub>2</sub>OH.HCl in 25% acetic acid. The mixture was continuously shaken at 100 rpm for 5 hours at 80°C.
- Step 4 (Bound to organic matter and sulfide minerals): The extractant of this step was the mixed solution of 20 ml of 0.04M NH<sub>2</sub>OH.HCl in 25% acetic acid, 8 ml of 30% H<sub>2</sub>O<sub>2</sub>, and 8 ml of 0.02 M HNO<sub>3</sub>, which was mixed with the residual soil sample from step 3 by shaking at 100 rpm for 5 hours at 80°C.
- Step 5 (Residual): 20 ml of HNO<sub>3</sub> 60% was used to dissolve all minerals containing As to recover total As in soils, and the mixture was boiled for 1 hour using a hot sand plate.

The mixture after shaking from step 1 to step 5 was centrifuged at a 3,000 rpm for 40 minutes using a centrifuge s300 series (Kubota Corporation, Japan). After centrifugation, the supernatant was decanted while the residues were washed with 10 ml of DI water. From step 1 to step 4, the supernatant was mixed with the “washing” water, and diluted to 50 ml, while those of step 5 was diluted to 100 ml. The diluted solutions were filtered by using 0.45  $\mu\text{m}$  Millex® membrane filters, which were immediately analyzed for As by ICP-AES-HVG.

The sequential extraction was applied for original soil samples and samples with cement to observe change in phases of As. The extraction experiments were done in triplicates for more accuracy and reliability.

### **3.3 Results and Discussion**

#### ***3.3.1 Properties of soil samples***

Table 3.1 shows the identified minerals and the types of original soil samples. The soil samples were categorized into sandy loam (A), silty loam (B, C, D and E), silt (F and H), and sand (G). The minerals with very high, high, and medium abundances are considered as major minerals. Major minerals were quartz ( $\text{SiO}_2$ ), cristobalite ( $\text{SiO}_2$ ), anorthite ( $\text{CaAl}_2\text{Si}_2\text{O}_8$ ) and albite ( $\text{NaAlSi}_3\text{O}_8$ ). Trace amounts of pyrite ( $\text{FeS}_2$ ) were detected in all soil samples tested while minor amounts of muscovite ( $(\text{K,Al})_2(\text{AlSi}_3\text{O}_{10})(\text{FOH})_2$ ) were detected in Samples F and G. Kaolinite ( $\text{Al}_2\text{Si}_2\text{O}_5(\text{OH})_4$ ) was also detected in Sample H. Meanwhile, mineral compositions of the soil samples with cement addition were also evaluated by XRD analysis. The results showed that XRD patterns of soil with and without cement addition were the same. This means that new minerals formed by cement addition were not detected by XRD whereas the identified minerals in the original soils were also detected in the soils with cement.

Table 3.2 lists the chemical compositions of soil samples. The major chemical compositions of the soils were  $\text{SiO}_2$ ,  $\text{Al}_2\text{O}_3$ , and  $\text{Fe}_2\text{O}_3$ , irrespective of soil type. The original soil samples contained 14 to 494 mg/kg of As. The contents of As in these soils were higher than the average As content in the Earth’s crust of about 1 mg/kg (Drahota and Filippi, 2009). In particular, the contents of As in Samples C, D, and F were much higher than the average content of As of the Earth’s crust, which could be attributed to

volcanic and marine sedimentary origin of the precursor rocks and sediments that formed these soils. Sapporo is located in the volcanic front of northeast Japan where As distribution is remarkably high as illustrated in the As geochemical map of Japan (Imai et al., 2004).

In Table 3.2, the chemical compositions of the mixture of soil and cement are also shown. For example, A0.3 means the mixture of 1 g Sample A and 0.003 g (0.3%) of cement. The content of CaO of Samples A, D, and F increased with increasing percentage of cement addition because the main component of cement is CaO.

### 3.3.2 Batch leaching experiments without cement addition

The As leaching concentration from soils without cement is shown in Fig. 3.1. The As concentration from Samples C, D and F exceeded the drinking water standard (10 µg/L) whereas those from samples A, B, E, G, and H were lower than the standard. In particular, the As leaching concentrations from Samples C and D were higher than 100 µg/L. It was also observed that the As leaching concentration was related to the As content in soil and not the particle size.

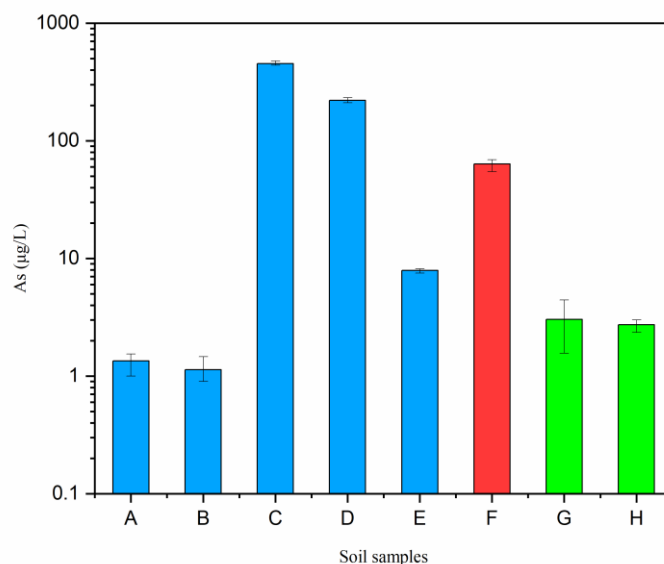


**Fig. 3.1.** Leaching concentration of As from soils without cement addition

Samples A, B, C, D, and E belong to borehole B1, Sample F belongs to borehole B2, and Samples G and H belong to borehole B3.

**Table 3.1.** Mineralogical properties and the types of soil samples tested

Sample	Borehole	Depth (m)	Type	Clay (<0.002 mm)	Silt (0.002-0.063 mm)	Sand (>0.063 mm)	Quartz	Cristobalite	Anorthite	Albite	Muscovite	Kaolinite	Pyrite
A	B-1	8.5–9.0	Sandy loam	1%	33%	66%	++	++	+++	+++			–
B	B-1	25.5–26.0	Silty loam	1%	59%	40%	++	++	+++	++			–
C	B-1	47.5–48.0	Silty loam	1%	54%	45%	++	++	+++	+++			–
D	B-1	48.0–48.5	Silty loam	0%	60%	40%	++	++	++++	+++			–
E	B-1	51.5–52.0	Silty loam	4%	56%	40%	+++	++	++++				–
F	B-2	21.5–21.85	Silt	4%	87%	9%	+++		++	+++	+		–
G	B-3	29.0–29.2	Sand	0%	2%	98%	+++		++++		+		–
H	B-3	29.8–30.0	Silt	4%	90%	6%	+++		+++			+	–

Notes: “++++” means very high (>50%); “+++” means high (30-50%); “++” means medium (10-30%); “+” means minor (5-10%); “–” means trace (<5%)

Match!® software could identify not only the minerals presented but also semi-quantitative abundance of minerals. The minerals with abundant percentages higher than 50% are generally considered very high whereas the minerals with abundant percentages belong to the ranges of 30-50%, 10-30%, and 5-10% are generally considered high, medium, and minor, respectively. Finally, the minerals with abundant percentage of just a few percent (<5%) are considered as trace minerals.



**Table 3.2.** Chemical compositions of soil samples tested

Sample	SiO <sub>2</sub> (wt%)	TiO <sub>2</sub> (wt%)	Al <sub>2</sub> O <sub>3</sub> (wt%)	Fe <sub>2</sub> O <sub>3</sub> (wt%)	MnO (wt%)	MgO (wt%)	CaO (wt%)	Na <sub>2</sub> O (wt%)	K <sub>2</sub> O (wt%)	P <sub>2</sub> O <sub>5</sub> (wt%)	S (wt%)	As (mg/kg)	TOC (wt%)	IC (wt%)
A	62.5	0.6	22.6	11.4	0.2	1.4	2.0	1.6	2.1	0.1	0.04	56	0.08	<0.01
A0.3	65.2	0.6	18.8	11.7	0.1	1.6	2.2	1.9	2.3	0.1	0.05	-	-	-
A1	60.3	0.6	17.4	12.6	0.1	1.4	2.6	1.7	2.3	0.1	0.06	-	-	-
B	65.5	0.6	25.3	8.0	0.1	0.9	1.4	1.0	1.0	0.1	0.03	45	0.03	<0.01
C	64.2	0.6	22.1	9.4	0.5	1.8	2.7	1.8	1.6	0.2	0.02	494	0.04	<0.01
D	62.5	0.6	21.9	8.0	0.3	1.6	3.5	2.1	1.4	0.1	0.02	242	0.02	<0.01
D0.5	66.6	0.6	20.1	7.8	0.2	1.8	4.0	2.4	1.5	0.1	0.03	-	-	-
D2	66.1	0.6	19.5	8.0	0.2	1.9	4.7	2.4	1.6	0.1	0.10	-	-	-
E	63.8	0.7	20.6	9.6	0.2	1.5	3.1	1.9	1.5	0.2	0.17	79	0.03	<0.01
F	64.1	0.7	19.6	7.1	0.1	1.4	1.0	1.0	1.3	0.1	0.18	113	2.26	0.06
F3	67.9	0.7	18.6	5.1	0.1	1.5	2.8	1.1	1.4	0.1	0.20	-	-	-
F4	66.8	0.6	18.3	5.2	0.1	1.5	3.1	1.1	1.4	0.1	0.21	-	-	-
G	60.8	1.0	16.9	6.2	0.1	2.3	2.8	1.6	1.8	0.1	0.94	25	0.21	<0.01
H	64.4	0.7	20.7	13.4	0.2	1.4	0.8	0.9	1.3	0.2	0.04	14	0.55	0.48

Notes: “-” means “not analyzed”; figures in the name of sample mean the percentage of cement addition to soil (for example, A0.3 means the percentage of cement addition to soil is 0.3%).

### 3.3.3 Batch leaching experiments with cement addition

Three soil samples—Samples A, D, and F—were selected for evaluating the effects of cement addition because As leaching concentration from Sample A was low, that from Sample D was high, and that from Sample F was found in-between these two samples. Arsenic leaching from rocks increases when conditions become more acidic or alkaline (Tabelin and Igarashi, 2009), thus, the experimental data of As leaching from soils would also depend on the pH.

Arsenic leaching from soil samples A, D, and F with cement as a function of pH is depicted in Fig. 3.2. Leaching concentration of As increased from pH 8 to pH 10.3, and the highest As leaching concentration was observed at around pH 10.3. Above pH 10.3, the leaching concentration of As decreased. This overall trend was observed, irrespective of the samples. This implies that leaching concentrations of As from these soils were strongly dependent on pH when cement was added. In Fig. 2, cubic polynomial was applied to the observed data. These polynomials obtained by the least-square method explain the leaching behavior of As from these soils with cement.

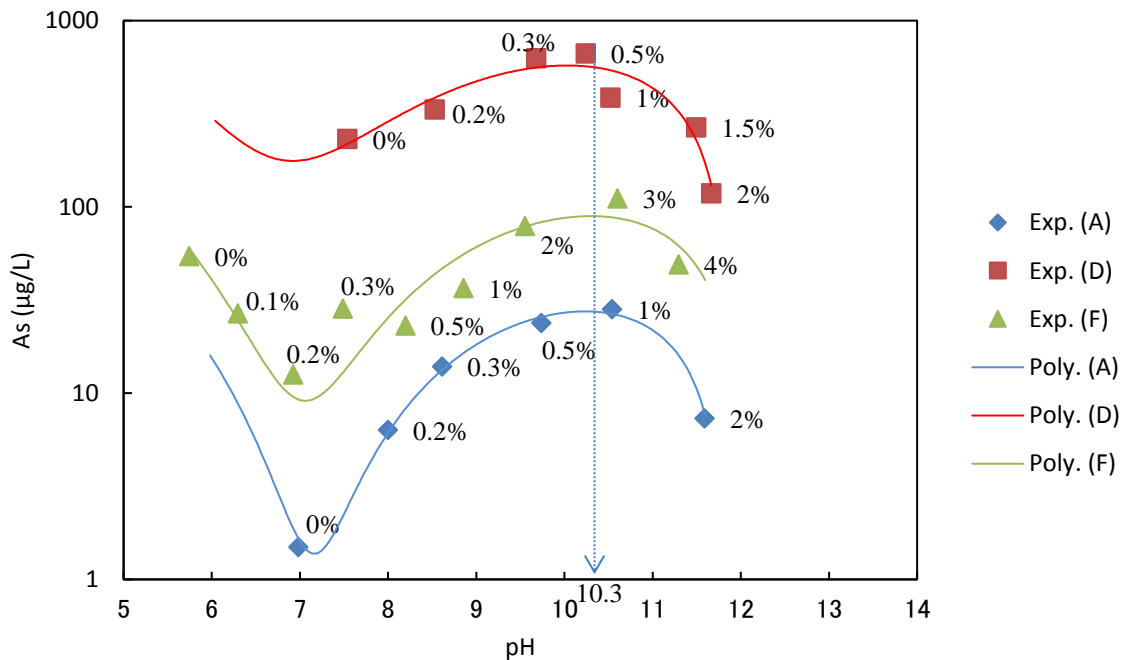


**Fig. 3.2.** The changes in leaching concentration of As versus pH with and without cement addition

The Eh-pH diagram predicts the predominant chemical species of elements with pH and redox potential of the system. Figure 3.3 shows that the major As species in the leaching solutions was  $\text{HAsO}_4^{2-}$ , which is a negatively charged oxyanion of arsenate (As(V)). This species is easily adsorbed onto positively charged surfaces as illustrated in Fig. 3.4. Negatively charged oxyanions of As(V) were adsorbed to the surfaces of Fe-oxyhydroxides/oxides (Igarashi et al., 2020; Tabelin et al., 2017a). The surface of Fe-oxyhydroxides/oxides has variable charges depending on pH. These minerals have zero charge at around pH 7. Meanwhile, they have positively charged surfaces at lower pH and negatively charged surfaces at higher pH. Thus, adsorption capacity decreases at alkaline pH, resulting in higher leaching concentration of As from pH 8 to pH 10.3. Above pH 10.3,  $\text{Ca}^{2+}$  is more abundant (Fig. 3.4(b)) and may enhance the adsorption of the negatively charged  $\text{HAsO}_4^{2-}$  by making the surface of Fe-oxyhydroxides/oxides more positive. The adsorption of As to Fe-oxyhydroxides is enhanced by  $\text{Ca}^{2+}$  via two mechanisms (Meng et al., 2002; Stachowicz et al., 2008; Tabelin et al., 2012b; Wilkie and Hering, 1996): (1) formation of more positively charged mineral surfaces, and (2) lower competitive effects of certain anions (e.g.,  $\text{HCO}_3^-$  and  $\text{CO}_3^{2-}$ ). Furthermore, with the increasing CaO contents in the soil samples with cement (Table 3.2) and the presence of sulfate ( $\text{SO}_4^{2-}$ ), the precipitation of  $\text{CaSO}_4$  is thermodynamically favorable. The partial sulfate was then replaced in ettringite precipitation at pH higher than around 10.3 (Mahedi et al., 2019). In the present study, the partial sulfate may be replaced by As(V), which results in reduction of As leaching concentration due to co-precipitation with Ca as  $\text{Ca}(\text{HAsO}_4)\text{SO}_4$ .

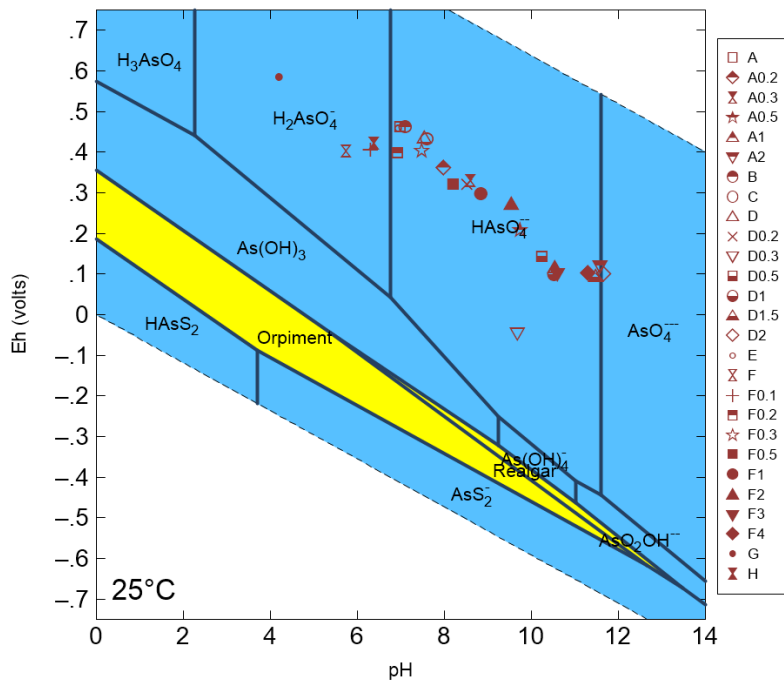
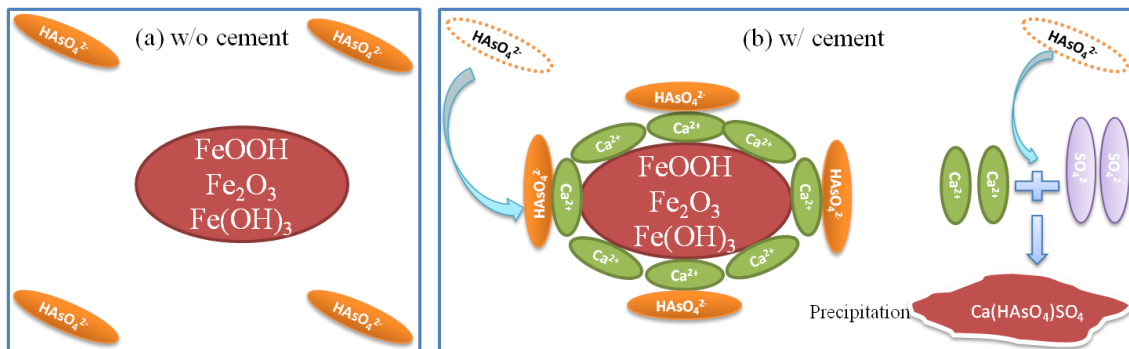


**Fig. 3.3.** Eh-pH predominance diagram of As at 25°C, 1.013 bar, activity of As =  $10^{-6}$ , activity of  $\text{SO}_4^{2-} = 10^{-3}$  and activity of  $\text{Ca}^{2+} = 10^{-4}$ . The diagram was created using the Geochemist's Workbench®.

$\text{HAsO}_4^{2-}$  was predicted as a major species of As in the leaching solutions.



Notes: “w/o cement” means “without cement”; “w/ cement” means “with cement”

**Fig. 3.4.** Schematic diagrams of As adsorption with and without cement

The surface charge of the functional group of Fe-oxyhydroxides/oxides is negative in the alkaline region. When  $\text{Ca}^{2+}$  is more abundant, it makes the surface of Fe-oxyhydroxides/oxides more positive by attaching surrounding due to electrical affinity.

HAsO<sub>4</sub><sup>2-</sup> ions are in the bulk solution, and they were then electrostatically attracted to the positively charged surfaces.

### 3.3.4 Sequential extraction without cement

The results of sequential extraction experiments are shown in Fig. 3.5. Significant amounts of As of about 24% in Sample C, 26% in Sample D, 17% in Sample E, and 17% in Sample F were partitioned with the exchangeable fraction, which is easily released under normal geochemical conditions. Moreover, substantial amounts of As were also associated with the sulfides and organic phase in Samples C, D, E, and F. These results were consistent with the higher contents of sulfur in Samples F and G and higher contents of TOC in Samples C, D, and F.

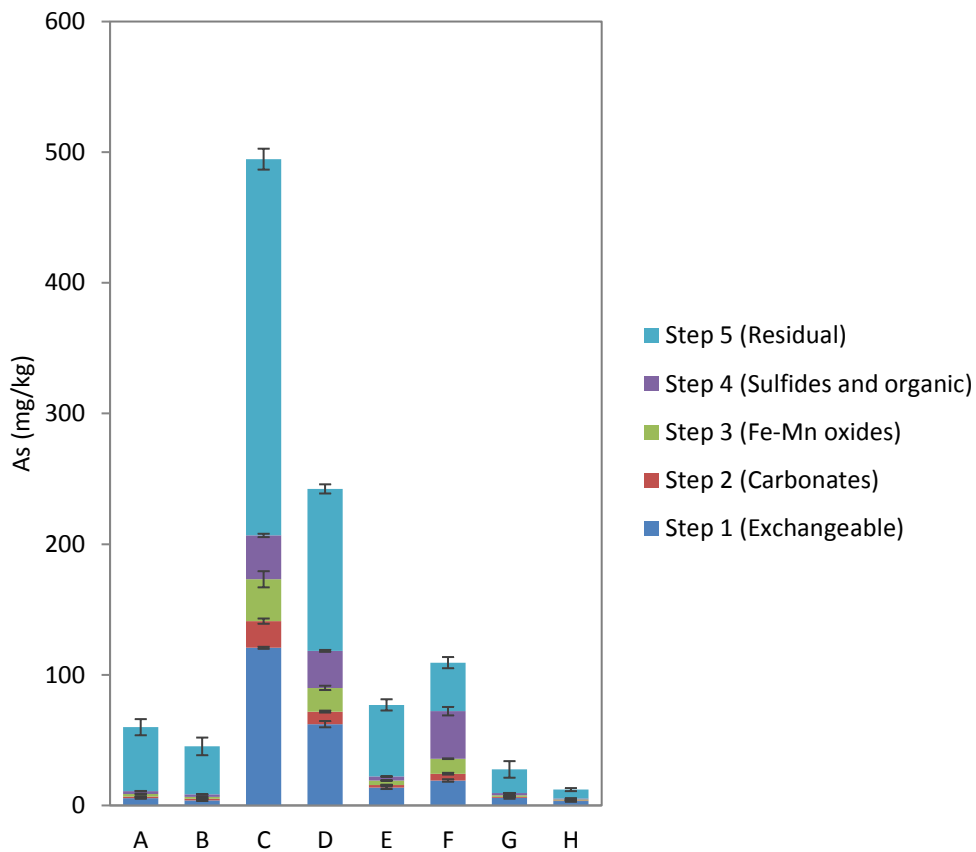


**Fig. 3.5.** Results of sequential extraction of original soil samples

(Substantial amounts of As in Samples C, D, E, and F were partitioned with the exchangeable fraction and the sulfides and organic fraction)

Arsenic leaching concentrations had a positive correlation with contents of exchangeable As and total As with the coefficient of determination of 0.99,  $p < 0.01$  (Figs. 3.6 and 3.7). The correlations between these three parameters indicate that leaching concentration of As was strongly influenced by exchangeable As content and total As content. In other words, leaching from the exchangeable As fraction is one of the major mechanisms affecting the release of As when cement is not added.

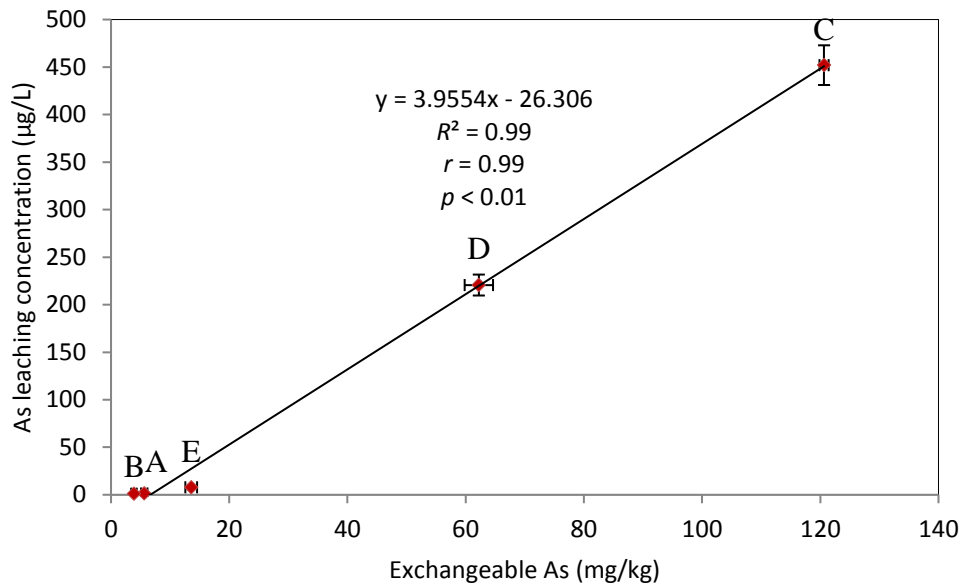


**Fig. 3.6.** Positive correlation between As leaching concentration and exchangeable As content

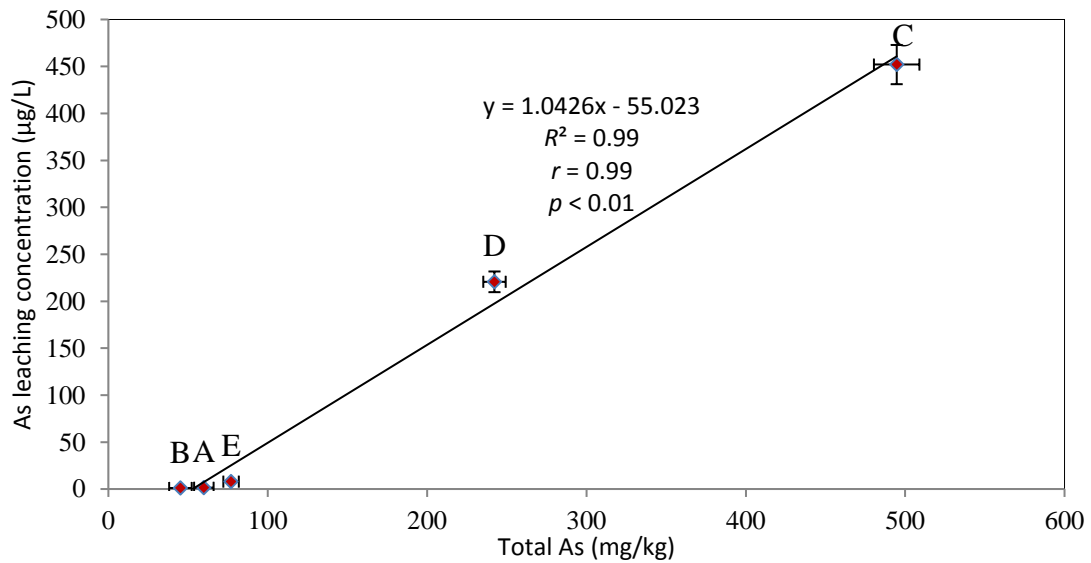


**Fig. 3.7.** Positive correlation between As leaching concentration and total As content

### 3.3.5 Sequential extraction with cement addition

After batch leaching tests, 1 g of Sample D, D0.3, and D1.5 was recovered to conduct sequential extraction in triplicates. Figure 3.8 shows the results of average values of each fraction. It is interesting to note that the exchangeable As phase did not change with the amount of cement added, suggesting that As leaching behavior might be unaffected by cement if the pH ranges from 7 to 11.5.

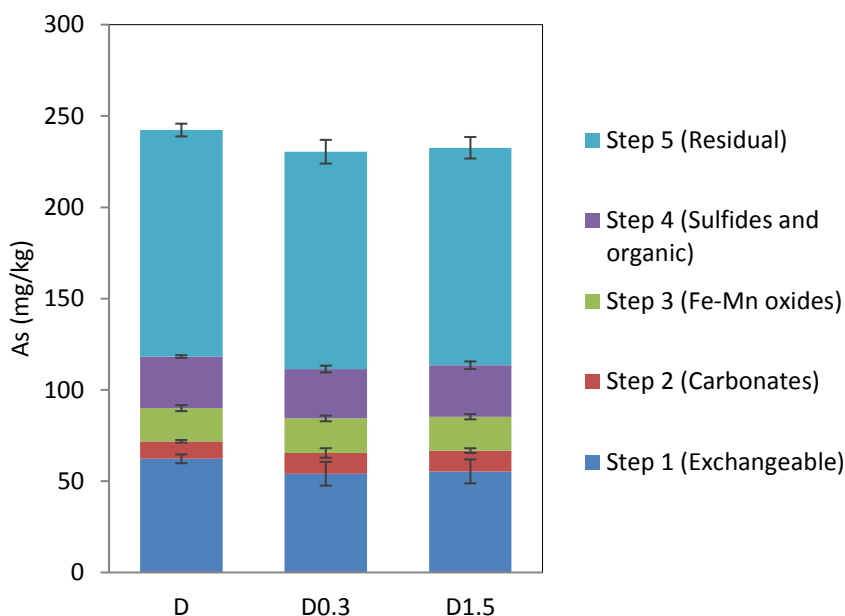
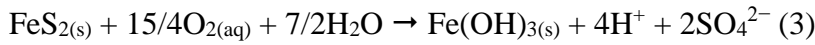
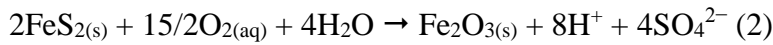
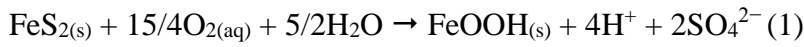


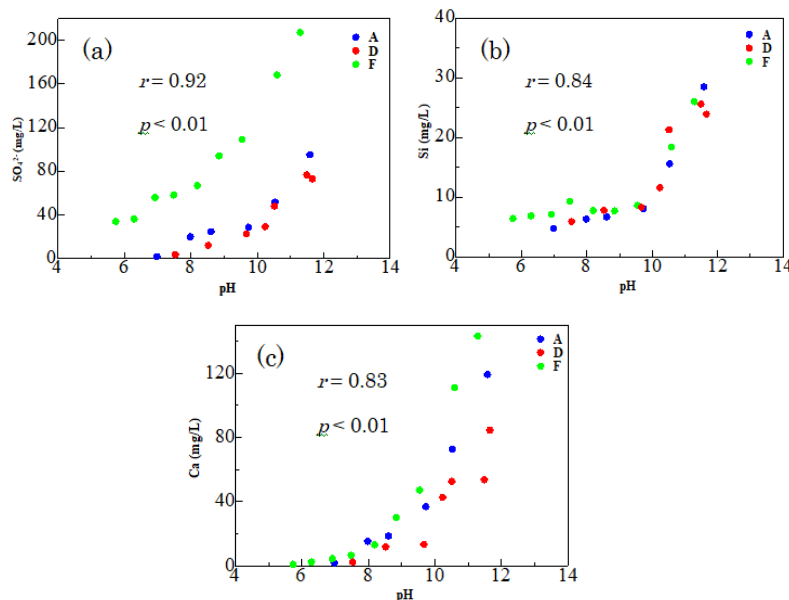
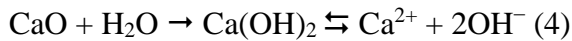
**Fig. 3.8.** Sequential extraction of Sample D without cement and with cement at 0.3 and 1.5% of soil

The leaching behavior of  $\text{SO}_4^{2-}$  was observed with both cationic and amphoteric leaching patterns (Mahedi et al., 2019, 2020). With a cationic leaching pattern, leaching concentration decreases with an increase of pH solution due to ettringite precipitation at pH higher than 10.7 (Mahedi et al., 2020) whereas with an amphoteric leaching pattern, minimum leaching concentration at neutral pH is expected due to adsorption and precipitation with  $\text{Al}(\text{OH})_3$  (Mahedi et al., 2019; Seng et al., 2019; Park et al., 2018, 2020). In the present study, the  $\text{SO}_4^{2-}$  concentration increased with pH as shown in Fig. 9(a) (correlation coefficient ( $r$ ) = 0.92,  $p < 0.01$ ), which could be attributed to the enhancement of pyrite oxidation with pH. The oxidation of pyrite under alkaline conditions can be described by the following reactions depending on the

chemical species of Fe-oxyhydroxides/oxides, which is a significant mechanism of As release in the alkaline region (Tabelin and Igarashi, 2009; Tabelin et al., 2017b, c).



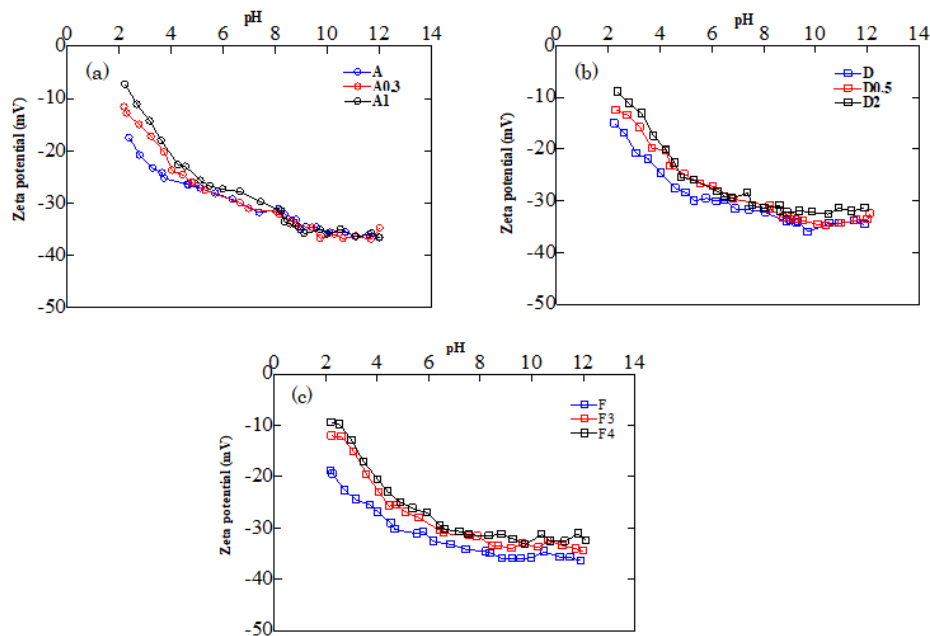
Both dissolved Si and  $\text{Ca}^{2+}$  concentrations increased with pH, indicated by the positive correlation coefficients of 0.84 and 0.83, respectively, at the 0.01 significance level, as shown in Figs. 3.9(b) and 3.9(c). In spite of the fact that  $\text{Ca}^{2+}$  concentrations usually decrease with an increase in pH in alkaline condition due to the precipitation of carbonates,  $\text{Ca}^{2+}$  concentrations increased in solution, since a significant amount of Ca from cement was dissolved in DI water as described in Eq. (4). The anionic species of dissolved Si under alkaline conditions interfere with As adsorption (Camacho et al., 2009; Huyen et al., 2019a; Zhang et al., 2004) whereas the  $\text{Ca}^{2+}$  induces As adsorption as explained previously. Thus, both elements may affect the leaching of As in excavated soils strengthened by cement.



**Fig. 3.9.** Positive correlations of leaching concentrations of  $\text{SO}_4^{2-}$  (a), Si (b), and Ca (c) with pH

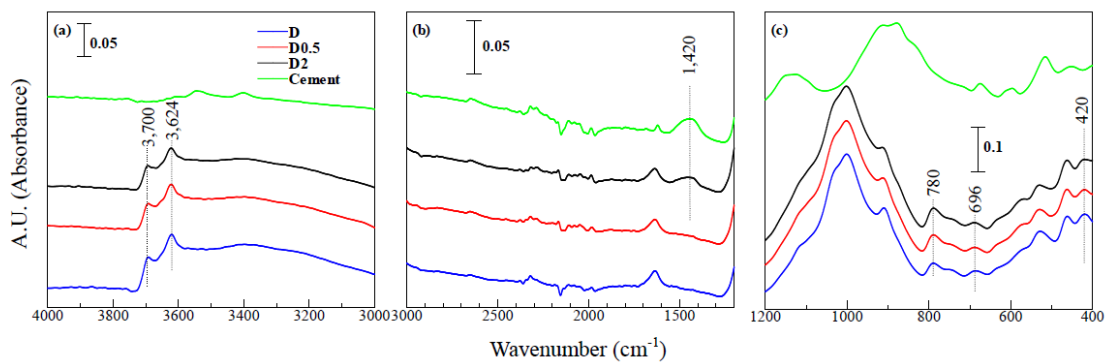


Figure 3.10 shows the zeta potential of soils versus pH. The t-tests in two pH regions for Samples A, D, and F with and without cement were performed to examine the differences of zeta potentials depending on the addition of cement. The results showed that the  $p$ -values, in case of testing Samples A and D, were less than 0.01 in the acidic region, while they were higher than 0.01 in the alkaline pH region. In addition, that of testing Sample F were less than 0.01 in both acidic and alkaline regions. These indicate that, in the acidic region, zeta potentials were significantly different depending on the addition of cement. Meanwhile, zeta potentials in the alkaline region were almost the same with and without cement, except Sample F since a significant amount of cement was added. These properties are explained by the amount of HCl added to the suspension of the mixture of soil and cement by pH adjustment. Higher volume of HCl solution was added when the mixing ratio of cement increased due to higher buffer capacity. The higher electrolyte reduces the electrical double layer, leading to higher zeta potential. In the alkaline region, the amounts of HCl added did not vary substantially. Thus, the zeta potential of the suspension did not change dramatically depending on the mixing ratio of cement. However, significant increase in the zeta potential was observed in samples D and F. This is due to cationic Ca adsorption to the soil.



**Fig. 3.10.** The changes in zeta potential versus pH of Sample A (a), Sample D (b), and Sample F (c) with and without cement

ATR-FTIR was applied to the soils with and without cement to characterize the effects of cement addition on the soil surface (Fig. 3.11). Trace amount of pyrite was detected by XRD that is further implied by the presence of S—S IR absorption bands ( $420\text{ cm}^{-1}$ ) (Tabelin et al., 2017c). Two absorption bands at  $780$  and  $696\text{ cm}^{-1}$  are assigned to Si—O vibrations of quartz and albite (Chen et al., 2014). In addition, the absorption bands at  $3,700$  and  $3,624\text{ cm}^{-1}$  are also assigned to O—H vibrations of quartz and albite (Chen et al., 2014). The absorption band at  $1,420\text{ cm}^{-1}$  is assigned to C—O vibrations of calcite (Andersen and Brečević, 1991; Tabelin et al., 2017d), which were detected in Sample D2, and not in Samples D and D0.5. This indicates that calcite was formed due to a significant amount of cement added. This means that ATR-FTIR can detect more sensitively the formation of Ca-bearing minerals compared to the XRD analysis.



**Fig. 3.11.** The changes in ATR-FTIR of Sample D with and without cement, absorption bands (a) from  $3,000$  to  $4,000\text{ cm}^{-1}$ , (b) from  $1,200$  to  $3,000\text{ cm}^{-1}$ , and (c) from  $400$  to  $1,200\text{ cm}^{-1}$

Based on these results, the leaching concentration of As in the soils increased after the addition of cement mainly because of the associated pH change rather than direct changes in the solid-phase partitioning of As in the soils. Moreover, newly formed minerals due to cement addition were not identified by XRD but changes in chemical bonding patterns were observed by ATR-FTIR.

### 3.4 Conclusion

The effects of cement addition on As leaching from soils were evaluated in the present study and the findings are summarized as follows:

- (1) Leaching concentrations of As had a positive correlation with the contents of exchangeable phase As and total As when cement did not added.
- (2) Leaching concentration of As from soils depended on pH adjusted by changing the amount cement addition. The maximum leaching concentrations of As were observed at pH 10.3, and the concentrations decreased when the pH was less than 10.3 and higher than 10.3.
- (3) The change in the properties of soil surface was detected by ATR-FTIR but not by XRD and sequential extraction.
- (4) As leaching may be restricted by pH adjustments by considering the properties of soils.

## References

- Abollino, O., Giacomino, A., Malandrino, M., Mentasti, E., Aceto, M., Barberis, R., 2006. Assessment of metal availability in a contaminated soil by sequential extraction. *Water, Air, & Soil Poll.*, 173(1-4), 315-338.
- Aguilar-Carrillo, J., Garrido, F., Barrios, L., García-González, M. T., 2009. Induced reduction of the potential leachability of As, Cd and Tl in an element-spiked acid soil by the application of industrial by-products. *Geoderma*, 149(3-4), 367-372.
- Andersen, F. A., Brečević, L., 1991. Infrared spectra of amorphous and crystalline calcium carbonate. *Acta Chem. Scand.*, 45(10), 1018-1024.
- Azhar, A. T. S., Azim, M. A. M., Aziman, M., Nabila, A. T. A., 2016. Leachability of arsenic (As) contaminated landfill soil stabilised by cement and bagasse ash. In *IOP Conference Series: Materials Science and Engineering* (Vol. 160, No. 1, 012078). IOP Publishing.
- Bethke, C. M., Yeakel, S., 2011. *The Geochemist's Workbench® – A User's Guide to GSS, Rxn, Act2, Tact, Spec8, React, Gtplot, X1t, X2t and Xtplot*. Aqueous Solutions LLC, Urbana, Illinois.
- Camacho, J., Wee, H. Y., Kramer, T. A., Autenrieth, R., 2009. Arsenic stabilization on water treatment residuals by calcium addition. *Journal of Hazardous Materials*, 165(1-3), 599-603.
- Casentini, B., Hug, S. J., Nikolaidis, N. P., 2011. Arsenic accumulation in irrigated agricultural soils in Northern Greece. *Sci. Total Environ.*, 409(22), 4802-4810.
- Chen, Y., Furmann, A., Mastalerz, M., Schimmelmann, A., 2014. Quantitative analysis of shales by KBr-FTIR and micro-FTIR. *Fuel*, 116, 538-549.
- Chiang, K. Y., Lin, K. C., Lin, S. C., Chang, T. K., Wang, M. K., 2010. Arsenic and lead (beudantite) contamination of agricultural rice soils in the Guandu Plain of northern Taiwan. *Journal of Hazardous Materials*, 181(1-3), 1066-1071.

- Delemos, J. L., Bostick, B. C., Renshaw, C. E., Stürup, S., Feng, X., 2006. Landfill-stimulated iron reduction and arsenic release at the Coakley Superfund Site (NH). *Environmental Science & Technology*, 40(1), 67-73.
- Dousova, B., Buzek, F., Lhotka, M., Krejcová, S., Boubinová, R., 2016. Leaching effect on arsenic mobility in agricultural soils. *Journal of Hazardous Materials*, 307, 231-239.
- Drahota, P., Filippi, M., 2009. Secondary arsenic minerals in the environment: a review. *Environment International*, 35 (8), 1243-1255.
- Farzan, S. F., Karagas, M. R., Chen, Y., 2013. In utero and early life arsenic exposure in relation to long-term health and disease. *Toxicology and Applied Pharmacology*, 272(2), 384-390.
- Frohne, T., Rinklebe, J., Diaz-Bone, R. A., Du Laing, G., 2011. Controlled variation of redox conditions in a floodplain soil: impact on metal mobilization and biomethylation of arsenic and antimony. *Geoderma*, 160(3-4), 414-424.
- Gersztyn, L., Karczewska, A., Gałka, B., 2013. Influence of pH on the solubility of arsenic in heavily contaminated soils. *Environmental Protection and Natural Resources*, 24(3), 7-11.
- Ghazvini, S. A., Tabrizi, M. A., Kobarfard, F., Baghban, A. A., Asgary, S., 2009. Ion release and pH of a new endodontic cement, MTA and Portland cement. *Iranian Endodontic Journal*, 4(2), 74.
- Ghosh, A., Mukiibi, M., Ela, W., 2004. TCLP underestimates leaching of arsenic from solid residuals under landfill conditions. *Environmental Science & Technology*, 38(17), 4677-4682.
- Ghosh, A., Mukiibi, M., Sáez, A. E., Ela, W. P., 2006. Leaching of arsenic from granular ferric hydroxide residuals under mature landfill conditions. *Environmental Science & Technology*, 40(19), 6070-6075.

- Gleyzes, C., Tellier, S., Astruc, M., 2002. Fractionation studies of trace elements in contaminated soils and sediments: a review of sequential extraction procedures. *TrAC Trends in Analytical Chemistry*, 21(6-7), 451-467.
- Huyen, D. T., Tabelin, C. B., Thuan, H. M., Dang, D. H., Truong, P. T., Vongphuthone, B., Kobayashi, M., Igarashi, T., 2019a. The solid-phase partitioning of arsenic in unconsolidated sediments of the Mekong Delta, Vietnam and its modes of release under various conditions. *Chemosphere*, 233, 512–523.
- Huyen, D. T., Tabelin, C. B., Thuan, H. M., Dang, D. H., Truong, P. T., Vongphuthone, B., Kobayashi, M., Igarashi, T., 2019b. Geological and geochemical characterizations of sediments in six borehole cores from the arsenic-contaminated aquifer of the Mekong Delta, Vietnam. *Data in Brief*, 104230.
- Igarashi, T., Imagawa, H., Uchiyama, H., Asakura, K., 2008. Leaching behavior of arsenic from various rocks by controlling geochemical conditions. *Miner. Eng.*, 21, 191-199.
- Igarashi, T., Herrera, S. P., Uchiyama, H., Miyamae, H., Iyatomi, N., Hashimoto, K., Tabelin, C. B., 2020. The two-step neutralization ferrite-formation process for sustainable acid mine drainage treatment: removal of copper, zinc and arsenic, and the influence of coexisting ions on ferritization. *Sci. Total Environ.*, 715, 136877.
- Imai, N., Terashima, S., Ohta, A., Ujiie-Mikoshihara, M., Okai, T., Tachibana, Y., Togashi, S., Matsuhisa, Y., Kanai, Y., Kamioka, H., Taniguchi, M., 2004. Geochemical map of Japan. Geological Survey of Japan, AIST, 209p. Japanese with English abstract. Available at: <https://gbank.gsj.jp/geochemmap>.
- Kalinowski, B. E., Oskarsson, A., Albinsson, Y., Arlinger, J., Ödegaard-Jensen, A., Andlid, T., Pedersen, K., 2004. Microbial leaching of uranium and other trace elements from shale mine tailings at Ranstad. *Geoderma*, 122(2-4), 177-194.
- Konda, T., 2001. Shield tunneling method. *Civil Engineering*, Japan Society of Civil Engineering, 39, 23-27.
- Koyama, Y., 2003. Present status and technology of shield tunneling method in Japan. *Tunnelling and Underground Space Technology*, 18, 145-159.

- Lee, S., 2006. Geochemistry and partitioning of trace metals in paddy soils affected by metal mine tailings in Korea. *Geoderma*, 135, 26-37.
- Li, J. S., Beiyuan, J., Tsang, D. C. W., Wang, L., Poon, C. S., Li, X. D., Fendorf, S., 2017. Arsenic-containing soil from geogenic source in Hong Kong: leaching characteristics and stabilization/solidification. *Chemosphere*, 182, 31-39.
- Mahedi, M., Cetin, B., Dayioglu, A. Y., 2019. Leaching behavior of aluminum, copper, iron and zinc from cement activated by fly ash and slag stabilized soils. *Waste Management*, 95, 334-355.
- Mahedi, M., Cetin, B., Dayioglu, A. Y., 2020. Effect of cement incorporation on the leaching characteristics of elements from fly ash and slag treated soils. *Journal of Environmental Management*, 253, 109720.
- Manzano, R., Silveti, M., Garau, G., Deiana, S., Castaldi, P., 2016. Influence of iron-rich water treatment residues and compost on the mobility of metal(loid)s in mine soils. *Geoderma*, 283, 1-9.
- Marove, C. A., Tangviroon, P., Tabelin, C. B., Igarashi, T., 2020. Leaching of hazardous elements from Mozambican coal and coal ash. *Journal of African Earth Sciences* 168, 103861.
- Marumo, K., Ebashi, T., Ujiie, T., 2003. Heavy metal concentrations, leachabilities and lead isotope ratios of Japanese soils. *Shigen-chishitsu*, 53(2), 125-146.
- Meng, X., Korfiatis, G. P., Bang, S., Bang, K. W., 2002. Combined effects of anions on arsenic removal by iron hydroxides. *Toxicol. Lett.*, 133, 103-111.
- Moon, D. H., Wazne, M., Yoon, I. H., Grubb, D. G., 2008. Assessment of cement kiln dust (CKD) for stabilization/solidification (S/S) of arsenic contaminated soils. *Journal of Hazardous Materials*, 159(2-3), 512-518.
- Neel, C., Bril, H., Courtin-Nomade, A., Dutreuil, J. P., 2003. Factors affecting natural development of soil on 35-year-old sulphide-rich mine tailings. *Geoderma*, 111(1-2), 1-20.

- O'Day, P. A., Vlassopoulos, D., Root, R., Rivera, N., 2004. The influence of sulfur and iron on dissolved arsenic concentrations in the shallow subsurface under changing redox conditions. *Proceedings of the National Academy of Sciences*, 101(38), 13703–13708.
- Ojovan, M. I. (Ed.), 2011. *Handbook of advanced radioactive waste conditioning technologies*. Elsevier.
- Park, I., Tabelin, C. B., Seno, K., Jeon, S., Ito, M., Hiroyoshi, N., 2018. Simultaneous suppression of acid mine drainage formation and arsenic release by carrier-microencapsulation using aluminum-catecholate complexes. *Chemosphere* 205, 414–425.
- Park, I., Tabelin, C. B., Seno, K., Jeon, S., Inano, H., Ito, M., Hiroyoshi, N., 2020. Carrier-microencapsulation of arsenopyrite using Al-catecholate complex: nature of oxidation products, effects on anodic and cathodic reactions, and coating stability under simulated weathering conditions. *Heliyon* 6, e03189.
- Pérez-de-Mora, A., Madrid, F., Cabrera, F., Madejón, E., 2007. Amendments and plant cover influence on trace element pools in a contaminated soil. *Geoderma*, 139(1-2), 1-10.
- Rahman, M. M., Ng, J. C., Naidu, R., 2009. Chronic exposure of arsenic via drinking water and its adverse health impacts on humans. *Environmental Geochemistry and Health*, 31(1), 189-200.
- Seng, S., Tabelin, C. B., Kojima, M., Hiroyoshi, N., Ito, M., 2019. Galvanic microencapsulation (GME) using zero-valent aluminum and zero-valent iron to suppress pyrite oxidation. *Mater. Trans.* 60 (2), 277–286.
- Silvetti, M., Castaldi, P., Holm, P. E., Deiana, S., Lombi, E., 2014. Leachability, bioaccessibility and plant availability of trace elements in contaminated soils treated with industrial by-products and subjected to oxidative/reductive conditions. *Geoderma*, 214, 204-212.
- Silwamba, M., Ito, M., Hiroyoshi, N., Tabelin, C.B., Hashizume, R., Fukushima, T., Park, I., Jeon, S., Igarashi, T., Sato, T., Chirwa, M., Banda, K., Nyambe, I., Nakata,



- H., Nakayama, S., Ishizuka, M., 2020. Recovery of lead and zinc from zinc plant leach residues by concurrent dissolution-cementation using zero-valent aluminum in chloride medium. *Metals*, 10(4), 531.
- Smedley, P. L., Kinniburgh, D. G., 2002. A review of the source, behavior and distribution of arsenic in natural waters. *Applied Geochemistry*, 17, 517-568.
- Stachowicz, M., Hiemstra, T., van Riemsdijk, W. H., 2008. Multi-competitive interaction of As(III) and As(V) oxyanions with  $\text{Ca}^{2+}$ ,  $\text{Mg}^{2+}$ ,  $\text{PO}_4^{3-}$ , and  $\text{CO}_3^{2-}$  ions on goethite. *J. Colloid Interface Sci.*, 320, 400-414.
- Tabelin, C. B., Igarashi, T., 2009. Mechanisms of arsenic and lead release from hydrothermally altered rock. *Journal of Hazardous Materials*, 169(1-3), 980-990.
- Tabelin, C. B., Igarashi, T., Tamoto, S., Takahashi, R., 2012a. The roles of pyrite and calcite in the mobilization of arsenic and lead from hydrothermally altered rocks excavated in Hokkaido, Japan. *J. Geochem. Explor.*, 119–120, 17–31.
- Tabelin, C. B., Igarashi, T., Takahashi, R., 2012b. Mobilization and speciation of arsenic from hydrothermally altered rock in laboratory column experiments under ambient conditions. *Appl. Geochem.*, 27, 326–342.
- Tabelin, C. B., Igarashi, T., Arima, T., Sato, D., Tatsuhara, T., Tamoto, S., 2014a. Characterization and evaluation of arsenic and boron adsorption onto natural geologic materials, and their application in the disposal of excavated altered rock. *Geoderma*, 213, 163–172.
- Tabelin, C. B., Hashimoto, A., Igarashi, T., Yoneda, T., 2014b. Leaching of boron, arsenic and selenium from sedimentary rocks: I. effects of contact time, mixing speed and liquid-to-solid ratio. *Sci. Total Environ.*, 472, 620–629.
- Tabelin, C. B., Hashimoto, A., Igarashi, T., Yoneda, T., 2014c. Leaching of boron, arsenic and selenium from sedimentary rocks: II. pH dependence, speciation and mechanisms of release. *Sci. Total Environ.*, 473, 244-253.
- Tabelin, C. B., Sasaki, R., Igarashi, T., Park, I., Tamoto, S., Arima, T., Ito, M., Hiroyoshi, N., 2017a. Simultaneous leaching of arsenite, arsenate, selenite, and

selenate, and their migration in tunnel-excavated sedimentary rocks: II. kinetic and reactive transport modeling. *Chemosphere*, 188, 444–454.

Tabelin, C. B., Veerawattananun, S., Ito, M., Hiroyoshi, N., Igarashi, T., 2017b. Pyrite oxidation in the presence of hematite and alumina: I. batch leaching experiments and kinetic modeling calculations. *Sci. Total Environ.*, 580, 687–689.

Tabelin, C. B., Veerawattananun, S., Ito, M., Hiroyoshi, N., Igarashi, T., 2017c. Pyrite oxidation in the presence of hematite and alumina: II. effects on the cathodic and anodic half-cell reactions. *Sci. Total Environ.*, 581–582, 126–135.

Tabelin, C. B., Sasaki, R., Igarashi, T., Park, I., Tamoto, S., Arima, T., Ito, M., Hiroyoshi, N., 2017d. Simultaneous leaching of arsenite, arsenate, selenite, and selenate, and their migration in tunnel-excavated sedimentary rocks: I. column experiments under intermittent and unsaturated flow. *Chemosphere*, 186, 558–569.

Tabelin, C. B., Igarashi, T., Tabelin, M. V., Park, I., Opiso, E. M., Ito, M., Hiroyoshi, N., 2018. Arsenic, selenium, boron, lead, cadmium, copper, and zinc in naturally contaminated rocks: a review of their sources, modes of enrichment, mechanisms of release, and mitigation strategies. *Sci. Total Environ.*, 645, 1522-1553.

Tamoto, S., Tabelin, C. B., Igarashi, T., Ito, M., Hiroyoshi, N., 2015. Short and long term release mechanisms of arsenic, selenium and boron from a tunnel-excavated sedimentary rock under in situ conditions. *J. Contam. Hydrol.*, 175, 60-71.

Tatsuhara, T., Arima, T., Igarashi, T., Tabelin, C. B., 2012. Combined neutralization–adsorption system for the disposal of hydrothermally altered excavated rock producing acidic leachate with hazardous elements. *Eng. Geol.*, 139, 76–84.

Tatsumi, K., Jin, K., Tachibana, H., 2006. Dynamic state of arsenic and basin management in Toyohira River, *Journal of Japan Society on Water Environment*, 29(11), 671-677.

Tchounwou, P. B., Centeno, J. A., Patlolla, A. K., 2004. Arsenic toxicity, mutagenesis, and carcinogenesis: a health risk assessment and management approach. *Molecular and Cellular Biochemistry*, 255(1-2), 47-55.

- Tessier, A., Cambell, G. C., Bisson, M., 1979. Sequential extraction procedure for the speciation of particulate trace metals. *Analytical Chemistry*, 51, 844-850.
- Wilkie, J. A., Hering, J. G., 1996. Adsorption of arsenic onto hydrous ferric oxide: effects of adsorbate/adsorbent ratios and co-occurring solutes. *Colloids Surf. A Physicochem. Eng. Asp.*, 107, 97-110.
- Yoon, I. H., Moon, D. H., Kim, K. W., Lee, K. Y., Lee, J. H., Kim, M. G., 2010. Mechanism for the stabilization/solidification of arsenic-contaminated soils with Portland cement and cement kiln dust. *Journal of Environmental Management*, 91(11), 2322-2328.
- Yun, S. W., Park, C. G., Jeon, J. H., Darnault, C. J., Baveye, P. C., Yu, C., 2016. Dissolution behavior of As and Cd in submerged paddy soil after treatment with stabilizing agents. *Geoderma*, 270, 10-20.
- Zhang, W., Singh, P., Paling, E., Delides, S., 2004. Arsenic removal from contaminated water by natural iron ores. *Miner. Eng.*, 17(4), 517-524.

## CHAPTER 4

### EFFECTS OF ADSORBENT ADDITION ON ARSENIC LEACHING FROM SHIELD-TUNNELING EXCAVATED SOILS

#### 4.1 Introduction

Underground facilities have been utilized widely since tunnel excavation is the first and important step of underground-facilities construction. When the facilities are constructed in the weak soil, shield-tunneling excavation is required due to its advantages in reinforcing the soft ground (Konda, 2001; Koyama, 2003). However, when this tunneling method is employed, it inadvertently changes the pH of environment, leading to more alkaline due to cement addition. In other words, it creates a favorable condition of As leaching. Therefore, countermeasures against As leaching should carefully be considered when the shield-tunneling excavation is adopted.

Irrespective of a variety of countermeasures of As leaching, adding adsorbents is one of the convenient methods. Various adsorbents have been used for As adsorption such as iron-oxide-coated diatomite (Pan et al., 2010), iron-oxide-coated cement (Kundu and Gupta, 2006), granular ferric hydroxide (Banerjee et al., 2008), iron oxide permeated mesoporous rice-husk nanobiochar (Nath et al., 2019), iron-rich industrial by-products (Lee et al., 2011), iron-based amendments (Naseri et al., 2014), pedogenic Fe–Mn nodule material (Chen et al., 2006), ferrihydrite (Zhang et al., 2019), steelmaking slag and limestone (Yun et al., 2016), untreated dolomite powder (Ayoub and Mehawej, 2007), iron oxide-coated sand (Gupta et al., 2005), natural iron oxide mineral (Aredes et al., 2013), lignite, bentonite, shale, and iron sand (Mar et al., 2013). Among them, magnesium oxide (MgO) and half-burnt dolomite (MgO.CaCO<sub>3</sub>) are reported as the effective adsorbents in the alkaline pH region (Tresintsi et al., 2014) whereas iron oxide adsorbent (Fe<sub>2</sub>O<sub>3</sub>) is often used for arsenate adsorption.

In the present study, the environment condition at the site is in the alkaline region; hence, these kinds of adsorbents were expected to work efficiently. Furthermore, they are considered as low-cost and easily available adsorbents (Salameh et al., 2015; Siddiqui and Chaudhry, 2017). Thus, there are a number of published researches about the effects of magnesium oxide, half-burnt dolomite, and iron oxide on As removal

from drinking water (Aredes et al., 2013), and seawater (Kameda et al., 2018). However, their performance on removal of As leached from shield-tunneling excavated soils is still not well understood. Therefore, the abilities of As adsorption from cement-bearing soils by magnesium oxide, half-burnt dolomite, and iron oxide were evaluated and compared. The outcomes of the present research suggest a promising adsorbent as well as the fundamental knowledge of the management of these alkaline excavated soils.

## **4.2 Materials and methods**

### **4.2.1 Materials used**

#### **4.2.1.1 Soil samples**

Three soil samples named A, D, and F were collected from a project of tunnel construction in Sapporo, Hokkaido, Japan. Geology of Sapporo mainly consists of soft alluvial deposits with high As distribution, which is highlighted in the research of Imai et al. (2004). As a result, As contained in soil samples A, D, and F are 56, 242, 113 mg/kg, respectively. These As contents are much higher than the natural background level, which is about 1 mg/kg (Drahota and Filippi, 2009). The core samples were transported to the laboratory, and were air-dried in the ambient conditions. After that, they were crushed and sieved to finer than 2 mm for batch leaching experiments.

#### **4.2.1.2 Cement**

The type of cement used for shield-tunneling excavation is selected depending on the compatibilities between the characteristics of cement and the characteristics of the excavation method. Shield-tunneling excavation method requires a cementitious type that rapidly hardens the walls of the excavated tunnel. In addition, that type of cement should easily be available, and low cost. Meanwhile, commercial ordinary Portland cement (OPC) fulfills all the above requirements since it has a high initial setting time and is used widespread at a low cost. Therefore, commercial OPC is considered as the suitable cement, which was also used in the present study. The main chemical compositions of the OPC are CaO with 63%, followed by SiO<sub>2</sub> with 21%, Al<sub>2</sub>O<sub>3</sub> with 5%, and Fe<sub>2</sub>O<sub>3</sub> with 5%.

#### ***4.2.1.3 Adsorbents***

Magnesium oxide called denite™, half-burnt dolomite, and iron oxide adsorbents were used in the present study. Chemical compositions of each adsorbent are shown in Table 4.1 by X-ray fluorescence analysis (XRF). Denite™ consisted of MgO as the main component with 74.8%. MgO contained in half-burnt dolomite with 17.6% was significantly lower than MgO in denite™. Meanwhile, CaO with 33.4% in the half-burnt dolomite was much higher compared to that of denite™ (0.55%). The highest-abundance chemical composition of half-burnt dolomite was the loss on ignition (LOI) with 46.8%, which is attributed to evaporation of CO<sub>2</sub> from calcium carbonate (CaCO<sub>3</sub>). The percentage of Fe<sub>2</sub>O<sub>3</sub> in iron oxide adsorbent amounted to 23.7%, which is considered as a main component. In addition, iron oxide adsorbent also contained a large amount of CaSO<sub>4</sub> (39.8%) and a few percent of Na<sub>2</sub>O.

#### ***4.2.1.3 Foam reagent and coagulant***

Commonly used foam reagent acts as a surfactant, which is used to fluidize soil particles. Meanwhile, commonly used coagulant is used to effectively separate soil particles and supernatant. Both foam reagent and coagulant are used in cases needed for enhancing the performance of excavation.

### ***4.2.2 Batch leaching experiments***

#### ***4.2.2.1 Batch leaching experiments without adsorbent***

For batch leaching experiments without adsorbent, 15 g of soil and 0.15 (1%), 0.075 (0.5%), and 0.3 g (2%) of cement for soil samples A, D, and F, respectively, were added to 150 ml of deionized (DI) water, to simulate soils excavated by the shield-tunneling method. Details of cases of batch leaching experiments are listed in Table 4.2. The percentages of cement were selected after several percentages of cement to soil were tested to observe the overall trend of As leaching, and these percentages of cement substantially changed the As leaching concentration. Meanwhile, the ratio between soil and DI water was selected based on Japanese standard on batch leaching test. The suspension was shaken at 120 rpm for 1 day. The supernatant was decanted, which was provided for pH, electrical conductivity (EC), and oxidation-reduction potential (ORP) measurements. The leachate was obtained by filtering the supernatant using 0.45 μm

Millex® membrane filters (Merck Millipore, USA). A certain volume of leachate after filtration was titrated with 0.01M sulfuric acid ( $H_2SO_4$ ) until pH 4.8. The rests of leachate were kept inside the refrigerator prior to chemical analysis. Alkalinity was then calculated from the results of titration. The concentrations of As were determined by using inductively coupled plasma atomic emission spectroscopy (ICP-AES) (ICPE-9000, Shimadzu, Corporation, Japan) with a hydride vapor generator (HVG) attachment while those of coexistence ions were measured by using the ICP-AES standard method. The batch leaching experiments without adsorbent were carried out in triplicate to obtain more accurate results.

**Table 4.1.** Chemical compositions of magnesium oxide (denite™), half-burnt dolomite, and iron oxide

Sample	SiO <sub>2</sub> (wt%)	TiO <sub>2</sub> (wt%)	Al <sub>2</sub> O <sub>3</sub> (wt%)	Fe <sub>2</sub> O <sub>3</sub> (wt%)	MnO (wt%)	MgO (wt%)	CaO (wt%)	Na <sub>2</sub> O (wt%)	K <sub>2</sub> O (wt%)	P <sub>2</sub> O <sub>5</sub> (wt%)	S (wt%)	LOI (wt%)
Magnesium oxide (Denite™)	0.18	<0.01	<0.01	0.11	<0.01	74.8	0.55	1.43	<0.01	<0.01	1.24	21.7
Half-burnt dolomite	0.09	<0.01	0.01	0.03	<0.01	17.6	33.4	<0.01	<0.01	<0.01	<0.01	46.8
Iron oxide	0.11	<0.01	0.08	23.7	2.19	0.62	39.8	0.21	<0.01	0.07	33.0	<0.01

\*Note: LOI means loss on ignition.



**Table 4.2.** Details of cases of batch leaching experiments

Category	Samples tested
Batch leaching experiments without adsorbent	A1, D0.5, F2
Batch leaching experiments with magnesium oxide addition	A1-0.2De, A1-0.5De, A1-1De, D0.5-0.2De, D0.5-0.5De, D0.5-1De, F2-0.2De, F2-0.5De, F2-1De
Batch leaching experiments with half-burnt dolomite addition	A1-0.2Do, A1-0.5Do, A1-1Do, D0.5-0.2Do, D0.5-0.5Do, D0.5-1Do, F2-0.2Do, F2-0.5Do, F2-1Do
Batch leaching experiments with iron oxide addition	A1-0.2Ir, A1-0.5Ir, A1-1Ir, D0.5-0.2Ir, D0.5-0.5Ir, D0.5-1Ir, F2-0.2Ir, F2-0.5Ir, F2-1Ir
Batch leaching experiments with foam reagent and coagulant addition	A1-FC, D0.5-FC, F2-FC

\*Note: The percentages of cement and adsorbents are marked via the name of samples. For example, D0.5-0.2Do means the mixture of 15 g of soil sample D, 0.5% (0.075 g) of cement, and 0.2% (0.03 g) of half-burnt dolomite. The expression is also applied for soil samples A and F, as well as the other adsorbents of magnesium oxide (De) and iron oxide (Ir).

D0.5-FC means the mixture of 15 g of soil sample D, 0.5% (0.075 g) of cement, 0.6 ml of foam reagent and 0.03 ml of coagulant. The expression is also applied for the other cases.

#### ***4.2.2.2 Batch leaching experiments with adsorbent***

For batch leaching experiments with adsorbent, a certain dose of cement and various doses of the adsorbents were added to soil. For soil sample A, fifteen grams of soil with 0.15 g (1%) of cement were mixed with 0.03 (0.2%), 0.075 (0.5%), and 0.15 g (1%) of adsorbents, respectively, in 150 ml of deionized (DI) water. For soil samples D and F, only the doses of cement were different compared with soil samples A, while the doses of adsorbents were the same. The doses of cement were 0.075 g (0.5%) for soil sample D and 0.3 g (2%) for soil sample F. The doses of cement were determined by considering the pH range whereas the doses of adsorbents were designed to observe the changes in As leaching depending on the amount of adsorbents added. After mixing, the remains of the procedure of batch leaching experiments with and without adsorbent were the same. The supernatant was decanted after shaking the suspension at 120 rpm for 1 day, which was provided for pH, EC, and ORP measurements. The leachate was then collected by filtered the supernatant. Alkalinity was also calculated from the results of titration. Arsenic leaching concentrations as well as coexistence ions concentrations were analyzed by using ICP-AES-HVG and ICP-AES, respectively. The batch leaching experiments with adsorbent were also conducted in triplicate to ensure that the observed trends are statistically significant.

#### ***4.2.2.3 Batch leaching experiments with foam reagent and coagulant***

In addition to cement, which is often added in shield-tunneling excavation for reinforcing the excavated tunnel walls, commonly used foam reagent and coagulant were also added when they were necessary to enhance the performance of excavation. Thus, in the laboratory experiments, the foam reagent and coagulant were added to mimic shield-tunneling excavation. For batch leaching experiments with foam reagent and coagulant, soil samples were also mixed together with a certain dose of cement and a certain volume of foam reagent and coagulant. In details, 15 g of soil with 0.15 (1%), 0.075 (0.5%), and 0.3 (2%) g of cement for soil samples A, D, and F, respectively, were mixed with 0.6 ml of foam reagent, and 0.03 ml of coagulant, in 150 ml deionized (DI) water. The volumes of foam reagent and coagulant were designed by considering the ratios of foam reagent, coagulant, and water at the site. After mixing, the rests of the procedure of batch leaching experiments with foam reagent and coagulant were the

same as those of batch leaching experiments with and without adsorbent. The mixture was also shaken at 120 rpm for 24 hours. The supernatant was then collected for measuring pH, EC, and ORP. The leachate was also obtained by filtering the supernatant, which used for measurements of alkalinity, As concentrations, and coexistent ion concentrations.

#### ***4.2.3 Characterization of soil samples***

X-ray powder diffraction (XRD) (MultiFlex, Rigaku Corporation, Japan), which identifies mineralogy, was used to characterize the original soil samples, and the samples with cement and adsorbent addition. In addition, the residuals of batch leaching experiments with adsorbents after decanted supernatants were collected and air dried at room temperature, followed by crushing to less than 50  $\mu\text{m}$ . The fine powders were then provided for attenuated total reflectance Fourier transform infrared spectroscopy (ATR-FTIR) (Jasco Analytical Instruments, Japan) to identify the differences in soil surfaces before and after adding the adsorbents.

#### ***4.2.4 Saturation index calculations***

The saturation indices of potential secondary minerals were calculated by using PHREEQC (Parkhurst and Apello, 1999), which are useful information in interpretation of dissolution/precipitation mechanisms. The input data were temperature, pH, redox potential (pe), concentrations of As and coexistence ions while minteq.v4.dat file was chosen as a thermodynamic database.

#### ***4.2.5 Geochemist's Workbench® model***

Arsenic could be existed as As (III) or As (V) in the solutions or precipitates as minerals, which depends on the geochemical conditions. Clarifying As species in the solutions helps better understanding the mechanisms of As release from shield-tunneling excavated soils affected by the addition of the adsorbents. Geochemist's Workbench® software (Bethke and Yeakel, 2011) was utilized to clarify chemical species of As. The input data were the activity of As and major ions, which were calculated by using PHREEQC.

#### **4.2.6 Principle component analysis (PCA)**

Principle component analysis is a technique of multivariate statistical analysis, which can show how meaningful relationships between variables, in particular, the correlations between As leaching concentration and the other variables are. Thus, the results of PCA could determine the important factors contributing to As leaching. Eleven parameters of 30 leachate samples were evaluated by using OriginPro 2020 software (OriginLab Corporation, USA).

### **4.3 Results and discussion**

#### **4.3.1 Properties of soil samples**

The composed minerals of soil samples A, D, and F with and without cement and adsorbent addition are shown in Fig. 4.1. The samples contained quartz ( $\text{SiO}_2$ ) and cristobalite ( $\text{SiO}_2$ ) as the highest-abundance minerals, while anorthite ( $\text{CaAl}_2\text{Si}_2\text{O}_8$ ) and albite ( $\text{NaAlSi}_3\text{O}_8$ ) were considered as the second-highest minerals, and muscovite ( $(\text{K,Al})_2(\text{AlSi}_3\text{O}_{10})(\text{FOH})_2$ ) was considered as a minor mineral and was detected in soil sample F only. Pyrite is commonly known as an As-containing mineral. It was detected in all samples as a trace mineral. It can be oxidized when exposed to the atmosphere, causing As leaching even in trace amounts (Schaufuß et al. 1998; Tangviroon et al., 2017), and thus it commonly contributes to higher As leaching. The minerals detected in original soil samples were also detected in the soil samples with cement and adsorbent addition, except a trace ettringite precipitation, which was detected in only soil samples with cement and adsorbent addition.

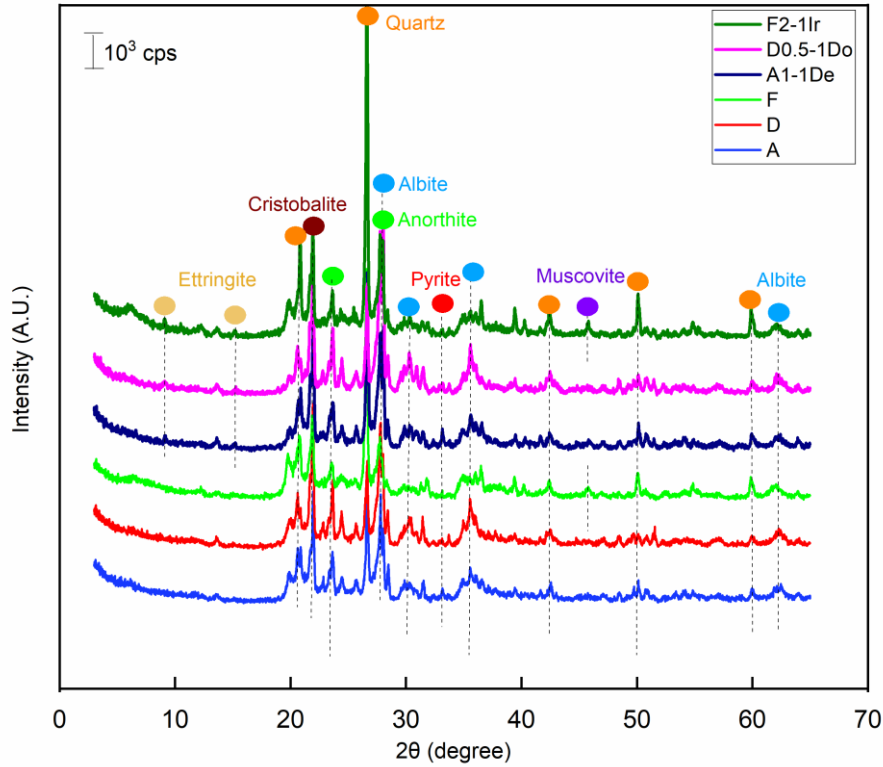


**Fig. 4.1.** The composed minerals of samples A, D, and F with and without cement and adsorbent addition

### 4.3.2 Batch leaching experiments with adsorbent

#### 4.3.2.1 Batch leaching experiments with magnesium oxide

Effects of addition of magnesium oxide on As leaching from soil samples A, D, and F are shown in Fig. 4.2. The leaching concentrations of As were decreased as the amount of adsorbent increased for all samples. Arsenic was removed by 73% and 66% from samples A and D at 1% magnesium oxide added, respectively. In particular, magnesium oxide reduced the As leaching of soil sample A to lower than drinking water standard 10  $\mu\text{g/L}$ . Meanwhile, As leaching decreased to 69% from soil sample F at 1% magnesium oxide addition. This indicates that magnesium oxide worked quite effectively in restricting As leaching from shield tunneling excavated soils.

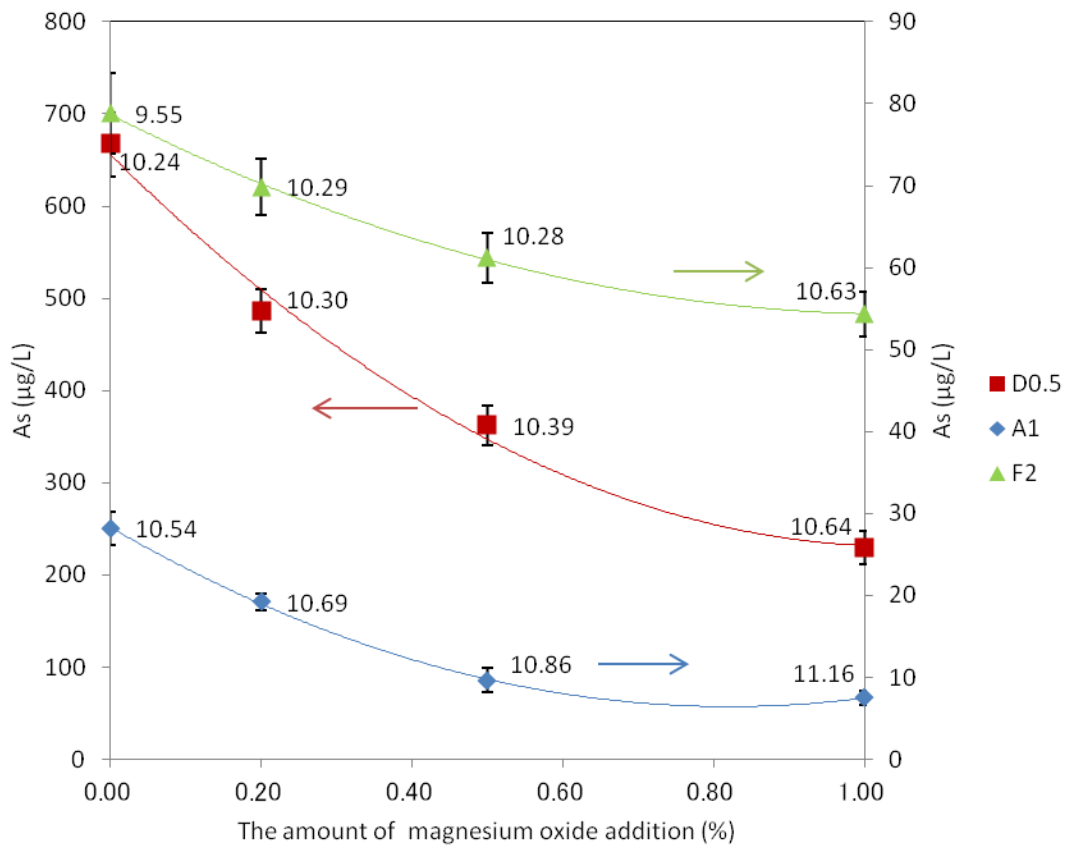


**Fig. 4.2.** Effects of addition of magnesium oxide on As leaching

\*Note: Figures beside symbols mean pH values in the leachate.

Left y-axis shows the leaching concentration of As in sample D while those of samples A and F are shown by right y-axis.

The addition of magnesium oxide slightly changed pH of the leachate, which can be explained by the following equation (Eq. 1)



The main component of the adsorbent is magnesium oxide (MgO), and pH was about 10.8 at 0.2 wt.% addition to DI water. When MgO reacts with DI water, anion hydroxide (OH<sup>-</sup>) is generated, which contributes to pH changes. This explanation is well supported by the results of Mg<sup>2+</sup> concentration as a function of amount of magnesium oxide added. The concentration of Mg<sup>2+</sup> generally increased with increasing of the amount of magnesium oxide as shown in Fig. 4.3. Consequently, the pHs of leachate

changed from 10.54 to 11.16, 10.24 to 10.64, and 9.55 to 10.63 for sample A, D, and F, respectively.

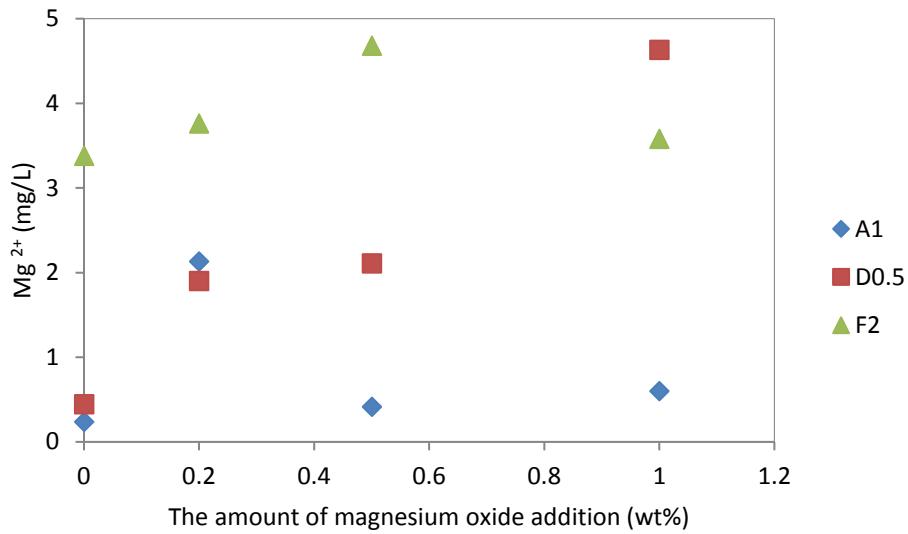


**Fig. 4.3.** Leaching concentration of  $Mg^{2+}$  versus the amount of magnesium oxide addition

Although the overall trend of concentration of  $Mg^{2+}$  increased with increasing amount of magnesium oxide,  $Mg^{2+}$  concentrations of samples A1-0.5De, A1-1De, and F2-1De were lower than those of A1-0.2De, and F2-0.5De. This happening is suspected. When  $Mg^{2+}$  is abundant due to magnesium oxide addition, the precipitation of possible Mg-minerals such as brucite ( $Mg(OH)_2$ ), dolomite ( $CaMg(CO_3)_2$ ), and/or magnesite ( $MgCO_3$ ) might occur. This assumption was confirmed by the results of saturation indices ( $SI$ ) of possible Mg-minerals (Table 4.3). The  $SI$ s of brucite of samples A1-0.5De and A1-1De were fell within the common error interval of saturation equilibrium ( $|SI| < 0.5$ ) whereas those of brucite and magnesite of sample F2-1De were also fell in the common error interval of saturation equilibrium.

**Table 4.3.** Saturation indices of possible Mg-minerals in leachate of batch leaching experiments with magnesium oxide addition

Sample	Brucite (Mg(OH) <sub>2</sub> )	Dolomite (CaMg(CO <sub>3</sub> ) <sub>2</sub> )	Magnesite (MgCO <sub>3</sub> )
A1	-2.12	0.91	-1.04
A1-0.2De	-1.09	1.71	<b>-0.30</b>
A1-0.5De	<b>-0.29</b>	0.63	-1.28
A1-1De	<b>-0.16</b>	0.81	-1.08
D0.5	-2.42	0.81	-0.84
D0.5-0.2De	-1.11	1.62	<b>-0.30</b>
D0.5-0.5De	<b>-0.32</b>	<b>0.33</b>	-0.70
D0.5-1De	-0.51	1.28	<b>-0.01</b>
F2	-2.97	1.12	<b>-0.25</b>
F2-0.2De	-0.89	2.59	<b>0.15</b>
F2-0.5De	-0.79	2.64	<b>0.24</b>
F2-1De	<b>-0.20</b>	2.43	<b>0.10</b>

\*Note: Values in bold numbers show saturation indices of the minerals falling into the common error interval of saturation equilibrium.

$|SI| < 0.5$ : the common error interval of saturation equilibrium

$SI < -0.5$ : the range of undersaturation

$SI > 0.5$ : the range of oversaturation

Schematic of As adsorption on the surface of Mg(OH)<sub>2</sub> and relevant co-precipitation as shown in Fig. 4.4 explains how effective magnesium oxide addition behaves to reducing As leaching because Mg(OH)<sub>2</sub> has a positively charged surface over the pH range measured (Tabelin et al., 2013). Meanwhile, in the present study, As exists as a negatively charged oxyanion of arsenate (As(V)) (HAsO<sub>4</sub><sup>2-</sup>), which was predicted by Geochemist's Workbench® (Fig. 4.5). Therefore, since Mg(OH)<sub>2</sub> and As(V) exist in the forms of opposite charges, it is easily attached to each other due to electrical affinity, thereby decreasing As leaching. In addition, Opiso et al. (2010) and Park et al. (2010) indicate that when the ratios by molar concentration between As(V) and Mg<sup>2+</sup> exceed 0.5 and the pHs range from 9 to 11, the precipitation of magnesium arsenate (Mg<sub>3</sub>(AsO<sub>4</sub>)<sub>2</sub>) could occur. However, in the present study, the molar ratios between As(V) and Mg<sup>2+</sup> were much lower than 0.5, thus, the precipitation of (Mg<sub>3</sub>(AsO<sub>4</sub>)<sub>2</sub>) might be excluded. Instead of that, Mahedi et al. (2019; 2020) figure out that pH > around 10.3 with abundance of Ca<sup>2+</sup> and SO<sub>4</sub><sup>2-</sup> is favorable for ettringite precipitation. Indeed, a trace ettringite mineral formed by cement and adsorbent



addition was detected by XRD in samples A1-1De, D0.5-1Do, and F2-1Ir (Fig. 4.1). Ettringite precipitation in the present study might occur via the following mechanisms;  $\text{CaSO}_4$  is first precipitated, and a part of  $\text{SO}_4^{2-}$  was then replaced by  $\text{As(V)}$  in the precipitation of  $\text{Ca}(\text{HAsO}_4)\text{SO}_4$ .

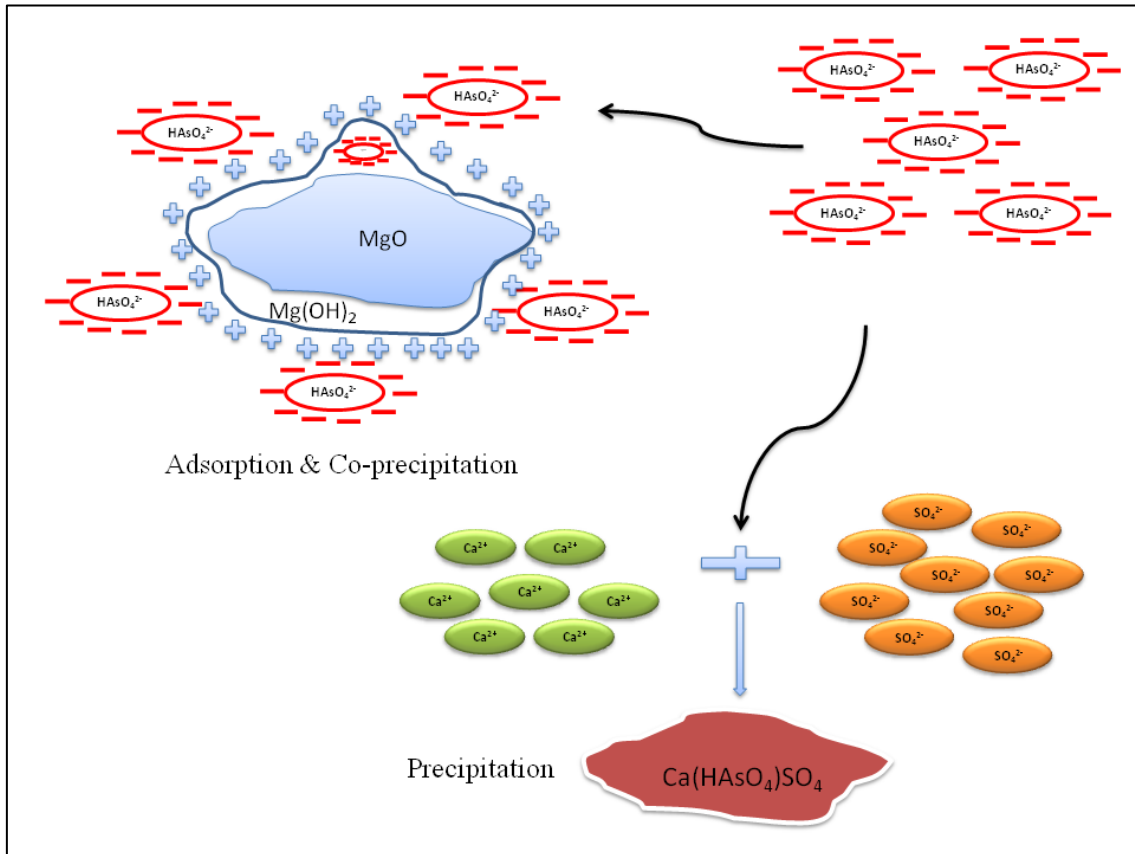


**Fig. 4.4.** Schematic diagram of As adsorption/precipitation/co-precipitation on magnesium oxide and half-burnt dolomite

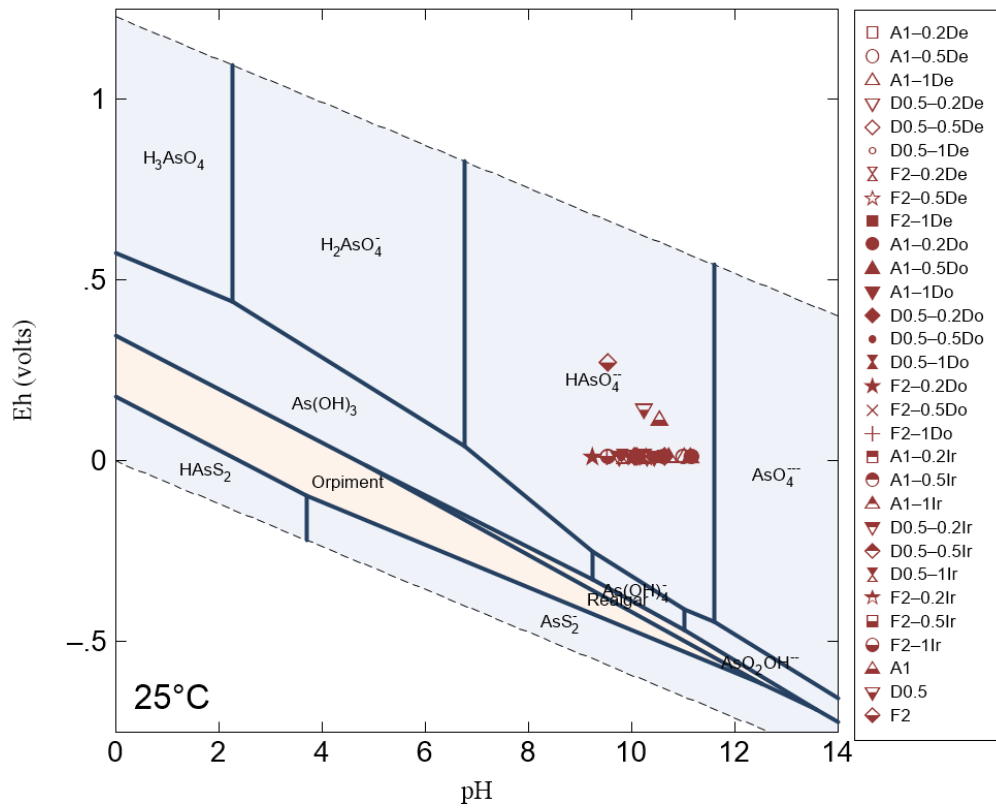
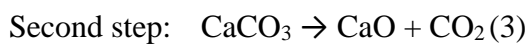
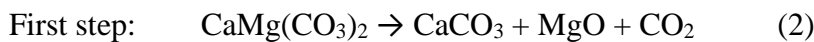


**Fig. 4.5.** Eh-pH predominance diagram of As at 25°C, 1.013 bar, activity of As =  $10^{-6}$ , activity of  $\text{SO}_4^{2-}$  =  $10^{-3}$  and activity of  $\text{Ca}^{2+}$  =  $10^{-3}$ . The diagram was created using the Geochemist's Workbench®.

#### 4.3.2.2 Batch leaching experiments with half burnt-dolomite

Half-burnt dolomite is produced by burning original dolomite ( $\text{CaMg}(\text{CO}_3)_2$ ) at  $750^\circ\text{C}$  for 2 hours, which can be obtained by stopping after the first step of two-step dolomite charring as expressed in the equation below (Eq. 2, 3) (Salameh et al., 2015). The adsorbent consists of magnesium oxide and calcium carbonate as the major components (Otsuka, 1986; Stefaniak et al., 2002). The pH of half-burnt dolomite is similar to magnesium oxide, which is also about 10.8 at 0.2 wt.% to DI water.



The slight changes in pH were also observed in case of half-burnt dolomite addition, similar to magnesium oxide. Anion  $\text{OH}^-$  is generated due to the reaction of  $\text{MgO}$  and DI water (Eq. 1), which could be confirmed via an increase of dissolved  $\text{Mg}^{2+}$  as a function of the amount of half-burnt dolomite addition (Fig. 4.6). The values of pH of the leachate changed from 10.54 to 10.92, 10.24 to 10.67, and 9.55 to 10.12 for soil samples A, D, and F, respectively. However, changes in pH by half-burnt dolomite addition were more moderate than by magnesium oxide addition. This is because coexisting calcium carbonate has a pH buffer capacity.

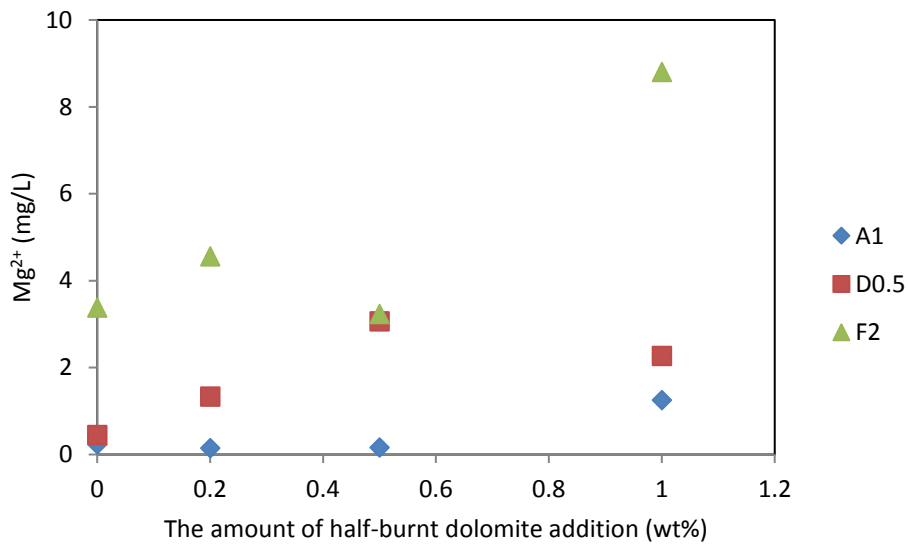


**Fig. 4.6.** Leaching concentration of  $\text{Mg}^{2+}$  versus the amount of half-burnt dolomite addition

Figure 4.7 illustrates the effects of half-burnt dolomite on As leaching from shield tunneling excavated soils. A significant amount (66%, 57%, and 36%) of As leaching from soil samples A, D, and F, respectively, was adsorbed at 1% half-burnt dolomite added. This means that half-burnt dolomite is also effective in adsorbing As. The more addition of half-burnt dolomite led to less As leaching.

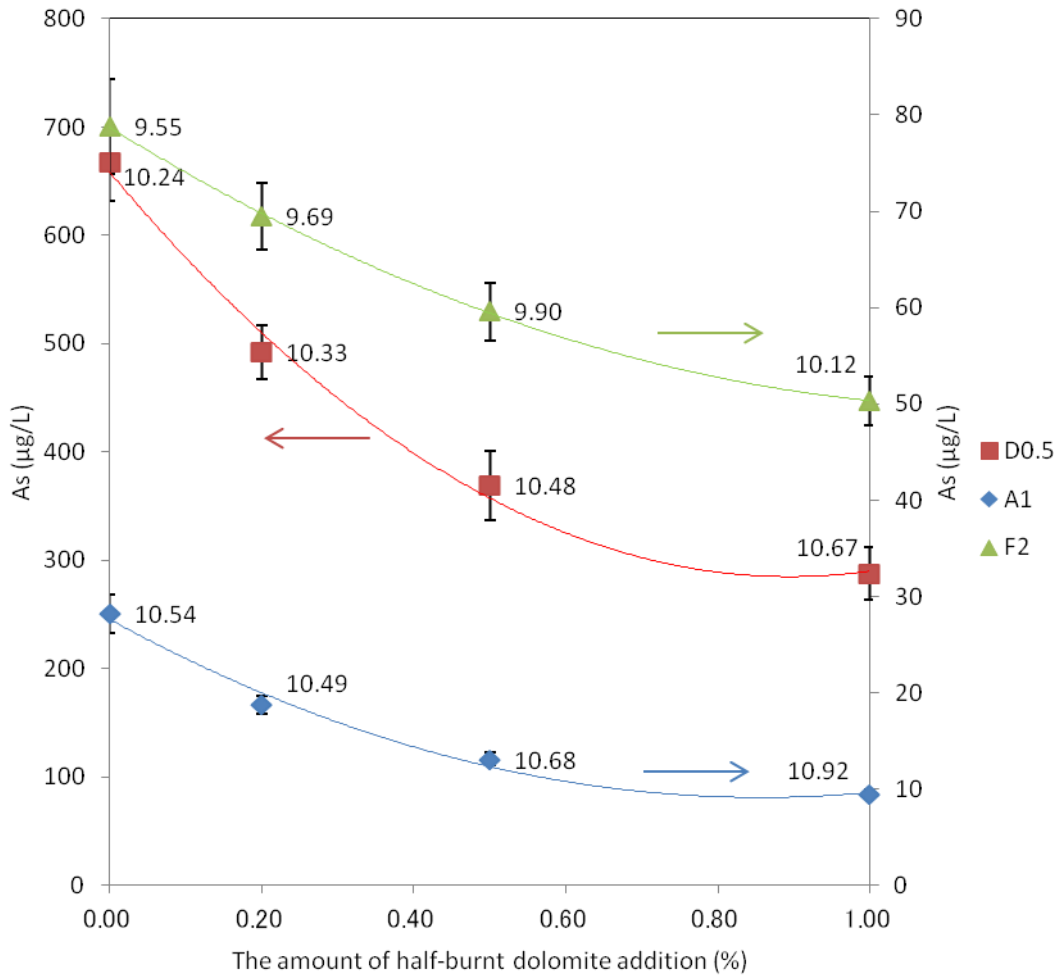


**Fig. 4.7.** Effects of addition of half-burnt dolomite on As leaching

\*Note: Figures beside symbols mean pH values in the leachate.

Left y-axis shows the leaching concentration of As in sample D while those of samples A and F are shown by right y-axis.

The mechanisms of As adsorption by adding half-burnt dolomite were similar to magnesium oxide addition (Fig. 4.4). The adsorption of As on the surface of  $Mg(OH)_2$  and co-precipitation of As in the precipitates  $Mg(OH)_2$  occurred. In addition, the molar ratios between As(V) and  $Mg^{2+}$  were also much lower than 0.5, and thus the co-precipitation of  $Mg_3(AsO_4)_2$  was not a main mechanism of reduction of As leaching in the present study. Moreover, the favorable pH condition along with the abundance of  $Ca^{2+}$  and  $SO_4^{2-}$  fulfilled the requirement for the ettringite precipitation.

#### 4.3.2.3 Batch leaching experiments with iron oxide

The pHs of the leachate were almost the same in case of iron oxide addition (Fig. 4.8). The maximum interval of pH change in the leachate of soil sample A was from 10.54 to 10.72, while that of soil sample D was from 10.24 to 9.93. For soil sample F, the pH of the leachate changed from 9.55 to 9.34. This is because  $\text{Fe}_2\text{O}_3$  did not change pH due to the low solubility in the alkaline pH region.

Figure 4.8 also describes the changes in As leaching with different amount of iron oxide addition. More iron oxide addition led to less As leaching. Arsenic was removed by 72%, 63%, and 42% at just only 1% iron oxide added for soil samples A, D, and F, respectively. Iron oxide was therefore quite effective in reducing As leaching from the excavated soils.

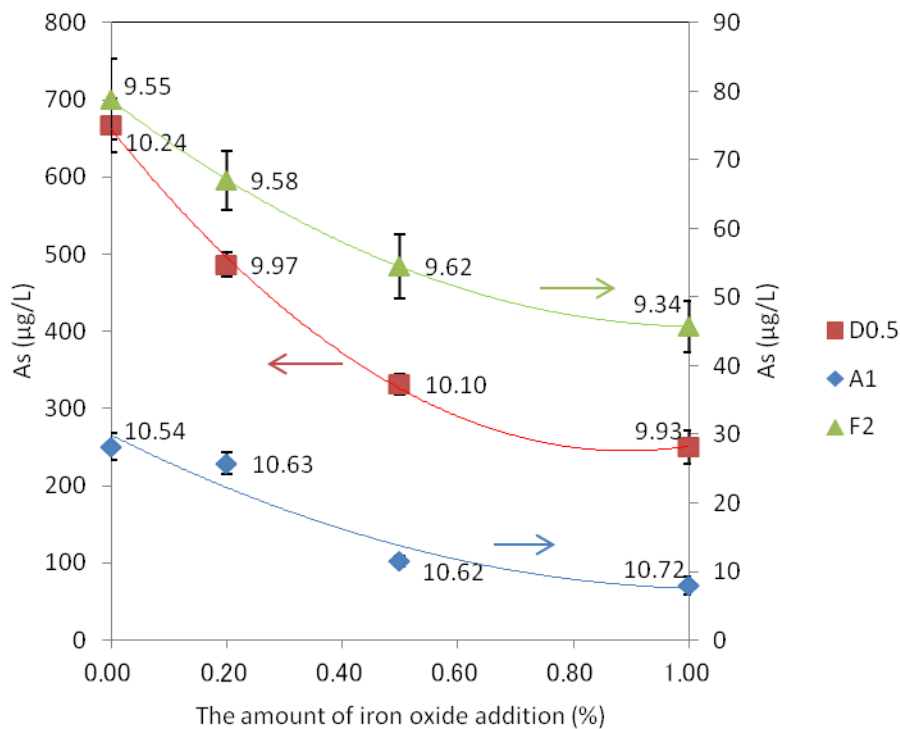
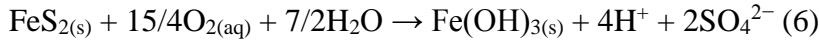
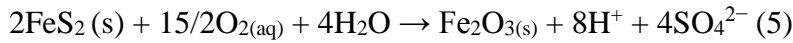
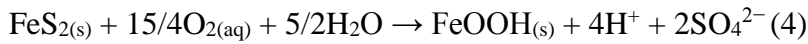


**Fig. 4.8.** Effects of addition of iron oxide on As leaching

\*Note: Figures beside symbols mean pH values in the leachate.

Left y-axis shows the leaching concentration of As in sample D while those of samples A and F are shown by right y-axis.

Concentrations of both dissolved  $\text{Ca}^{2+}$  and  $\text{SO}_4^{2-}$  increased as a function of amount of iron oxide addition as shown in Figs. 4.9 and 4.10. This result can be explained by considering the chemical compositions of iron oxide. The adsorbent consists of a large amount  $\text{CaSO}_4$  (39.8%). More amounts of the adsorbent resulted in more dissolved  $\text{Ca}^{2+}$  and  $\text{SO}_4^{2-}$ . However, at first, the molar ratio of  $\text{Ca}^{2+}$  and  $\text{SO}_4^{2-}$  versus the amount of iron oxide added was higher than 1 due to a large amount of dissolved  $\text{Ca}^{2+}$  from cement. The ratio was then decreased to lower than 1 (Fig. 4.11). This result from the fact that  $\text{SO}_4^{2-}$  was generated from dissolution of  $\text{CaSO}_4$  and consumed by the precipitation of Ca-bearing minerals. The presence of pyrite in the soil samples, which were detected by XRD, suggests that the increasing concentration of  $\text{SO}_4^{2-}$  might come from the pyrite oxidation, which is enhanced in alkaline pH region. (Tabelin and Igarashi, 2009).



In case of iron oxide addition,  $\text{pH} >$  around 10.3 together with abundance of  $\text{Ca}^{2+}$  and  $\text{SO}_4^{2-}$  is favorable conditions for ettringite precipitation, similar to magnesium oxide and half-burnt dolomite addition, which is one of the processes contributing to reducing As leaching.

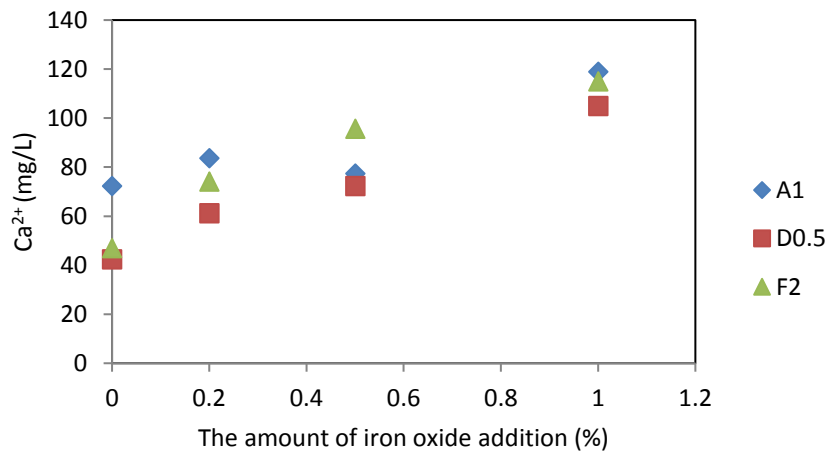


**Fig. 4.9.** Leaching concentration of  $\text{Ca}^{2+}$  versus the amount of iron oxide addition

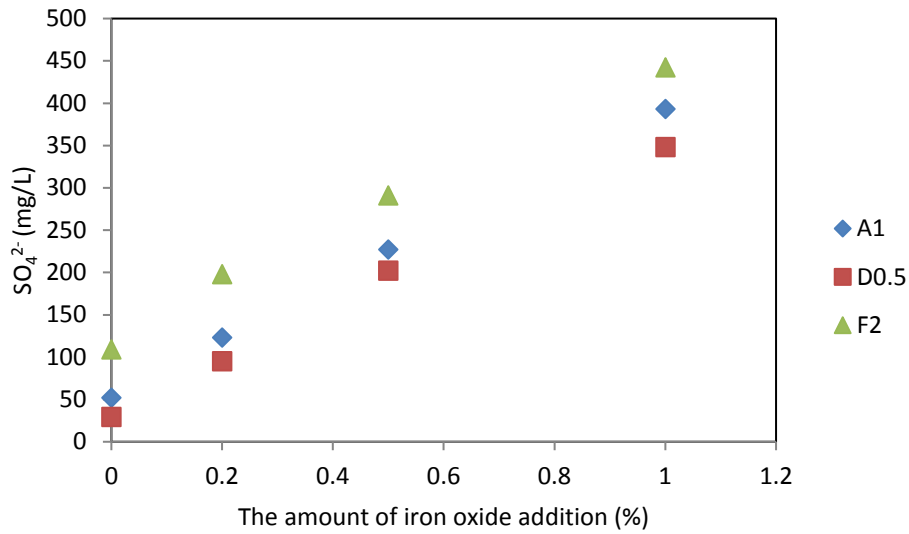


**Fig. 4.10.** Leaching concentration of  $\text{SO}_4^{2-}$  versus the amount of iron oxide addition

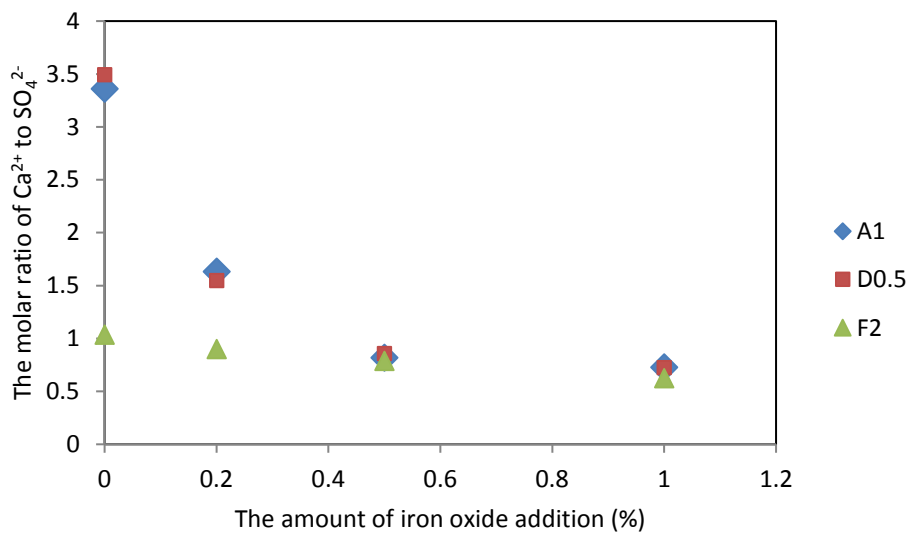


**Fig. 4.11.** The molar ratio of  $\text{Ca}^{2+}$  to  $\text{SO}_4^{2-}$  versus the amount of iron oxide addition

The mechanisms of As adsorption on iron oxide adsorbent are illustrated in Fig. 4.12 by considering the surface charge of  $\text{Fe}_2\text{O}_3$  and the competition between As and coexistence ions.  $\text{Fe}_2\text{O}_3$  has a negatively charged surface in the alkaline pH region. Meanwhile, the abundance of  $\text{Ca}^{2+}$  comes from not only iron oxide adsorbent addition but also cement dissolution.  $\text{Ca}^{2+}$  is then attached to the surface of  $\text{Fe}_2\text{O}_3$  due to electrical affinity, thereby the surface of  $\text{Fe}_2\text{O}_3$  becoming more positive. It creates a favorable condition for As adsorption since As exists as a negatively oxyanion of As(V). Besides, anions  $\text{HCO}_3^-$  and  $\text{CO}_3^{2-}$  have a positive relationship with As, which are shown

in Fig. 4.13. This suggests that when  $\text{HCO}_3^-$  and  $\text{CO}_3^{2-}$  become more abundant, they compete with As adsorbed on positive adsorption sites.

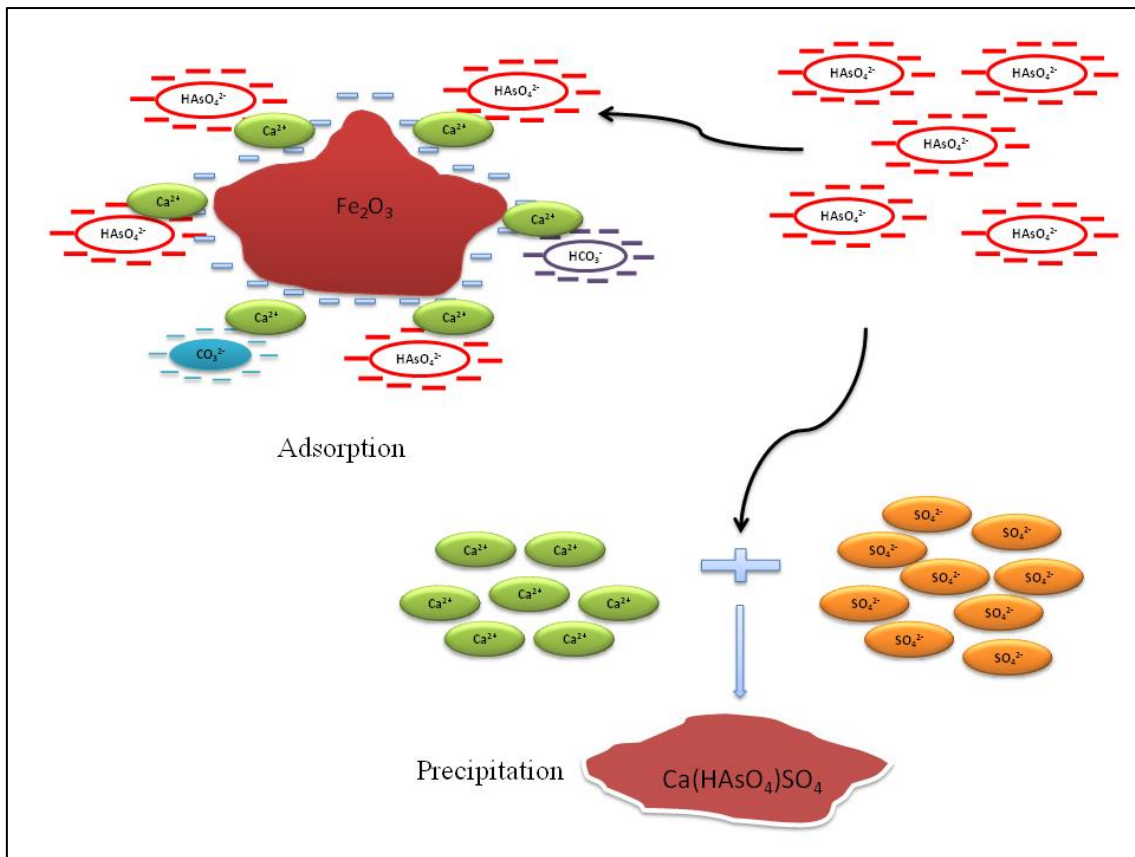


**Fig. 4.12.** Schematic diagram of As adsorption/precipitation on iron oxide



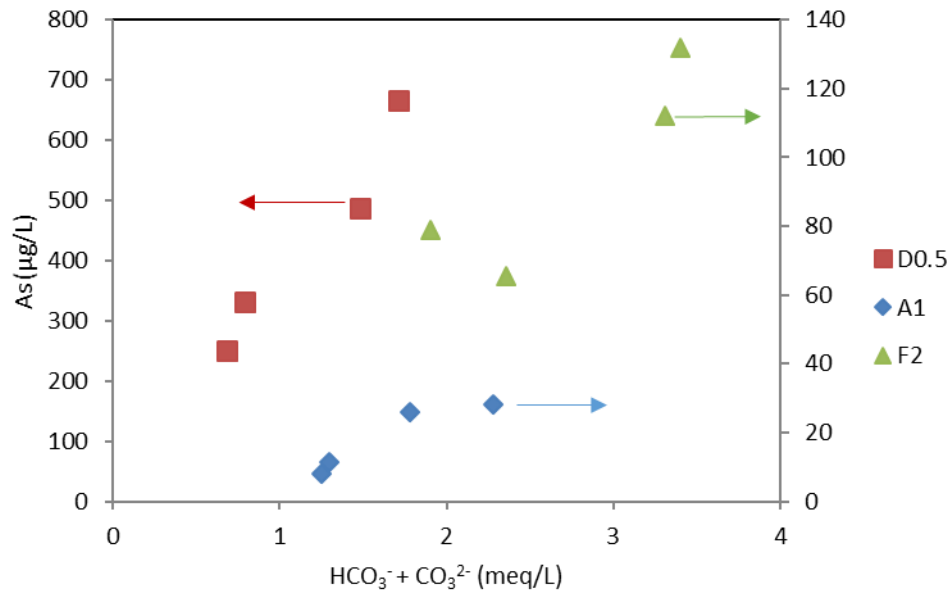


**Fig. 4.13.** Leaching concentration of As versus concentrations of  $\text{HCO}_3^-$  and  $\text{CO}_3^{2-}$  in case of iron oxide addition

\*Note: Left y-axis shows the leaching concentration of As versus alkalinity in sample D while those of samples A and F are shown by right y-axis.

#### 4.3.3 Performance of adsorbents

PCA results of the leaching experiments with magnesium oxide, half-burnt dolomite, and iron oxide addition are shown in Tables 4.4, 4.5, and 4.6, respectively. The As adsorption mechanisms could be confirmed by the results. The results of PCA in case of magnesium oxide addition and half-burnt dolomite addition are almost similar. The high loading of  $\text{Ca}^{2+}$  was attributed to the dissolved  $\text{Ca}^{2+}$  from cement addition, while high loading of  $\text{SO}_4^{2-}$  was attributed to pyrite oxidation. High loading of  $\text{Mg}^{2+}$  was the cause of the adsorbent addition since magnesium oxide and half-burnt dolomite consist of a significant amount of MgO. For PCA in case of iron oxide addition, high loadings of  $\text{Ca}^{2+}$  and  $\text{SO}_4^{2-}$  were attributed not only to cement addition and pyrite oxidation but also dissolution of  $\text{CaSO}_4$  from iron oxide addition. The second component accounted for 28% of variance with high loadings of pH, EC,  $\text{Ca}^{2+}$ ,  $\text{SO}_4^{2-}$ , and As, which attributed to the ettringite precipitation when  $\text{Ca}^{2+}$  and  $\text{SO}_4^{2-}$  were abundant in the alkaline condition (pH > around 10.3) (Mahedi et al., 2019), resulting in

reducing As leaching. Meanwhile, the third component accounted for 15% of variance with high loadings of  $\text{HCO}_3^-$  and  $\text{CO}_3^{2-}$ , and As, reflecting the fact that  $\text{HCO}_3^-$  and  $\text{CO}_3^{2-}$  were the competitive anions of As. Therefore, adsorption of As is the result of complex processes including competition between As and coexistence ions adsorbed onto the surfaces of  $\text{Mg}(\text{OH})_2$  and  $\text{Fe}_2\text{O}_3$ , and ettringite precipitation.

**Table 4.4.** Results of the principal component analysis in case of magnesium oxide addition

Parameters	PCA1	PCA2	PCA3
pH	-0.182	<b>0.460</b>	0.208
Eh	<b>0.336</b>	-0.260	-0.236
EC	<b>0.365</b>	0.205	0.099
$\text{HCO}_3^- + \text{CO}_3^{2-}$	<b>0.388</b>	0.111	-0.082
$\text{Ca}^{2+}$	<b>0.321</b>	0.273	-0.169
$\text{K}^+$	<b>0.347</b>	0.041	<b>0.395</b>
$\text{Mg}^{2+}$	0.263	<b>-0.334</b>	-0.137
$\text{Na}^+$	<b>0.347</b>	-0.138	<b>0.397</b>
$\text{SO}_4^{2-}$	<b>0.383</b>	0.159	-0.002
Si	-0.021	<b>0.539</b>	0.242
As	-0.098	<b>-0.380</b>	<b>0.682</b>
Eigenvalues	6.163	3.223	0.932
Percentage of variance (%)	56	29	8
Cumulative (%)	56	85	93

\*Note: Values in bold numbers show the parameters with high loadings.

**Table 4.5.** Results of the principal component analysis in case of half-burnt dolomite addition

Parameters	PCA1	PCA2	PCA3
pH	<b>-0.358</b>	0.258	0.105
Eh	<b>0.408</b>	-0.127	-0.044
EC	0.218	<b>0.422</b>	-0.181
HCO <sub>3</sub> <sup>-</sup> + CO <sub>3</sub> <sup>2-</sup>	0.170	<b>0.377</b>	<b>0.408</b>
Ca <sup>2+</sup>	-0.053	<b>0.484</b>	0.219
K <sup>+</sup>	<b>0.404</b>	0.096	0.178
Mg <sup>2+</sup>	<b>0.369</b>	-0.068	-0.195
Na <sup>+</sup>	<b>0.373</b>	-0.001	<b>0.419</b>
SO <sub>4</sub> <sup>2-</sup>	<b>0.324</b>	0.289	-0.185
Si	-0.286	<b>0.356</b>	0.150
As	-0.024	<b>-0.371</b>	<b>0.662</b>
Eigenvalues	5.532	3.872	1.034
Percentage of variance (%)	50	35	9
Cumulative (%)	50	85	94

\*Note: Values in bold numbers show the parameters with high loadings.

**Table 4.6.** Results of the principal component analysis in case of iron oxide addition

Parameters	PCA1	PCA2	PCA3
pH	<b>-0.331</b>	<b>0.313</b>	0.211
Eh	<b>0.371</b>	-0.198	0.214
EC	0.291	<b>0.395</b>	-0.114
HCO <sub>3</sub> <sup>-</sup> + CO <sub>3</sub> <sup>2-</sup>	0.208	-0.053	<b>0.652</b>
Ca <sup>2+</sup>	0.201	<b>0.463</b>	-0.186
K <sup>+</sup>	<b>0.354</b>	-0.148	<b>0.313</b>
Mg <sup>2+</sup>	<b>0.393</b>	0.027	-0.051
Na <sup>+</sup>	<b>0.402</b>	-0.038	0.008
SO <sub>4</sub> <sup>2-</sup>	0.266	<b>0.408</b>	-0.204
Si	-0.269	0.260	<b>0.422</b>
As	0.002	<b>-0.481</b>	<b>-0.341</b>
Eigenvalues	5.646	3.046	1.697
Percentage of variance (%)	51	28	15
Cumulative (%)	51	79	94

\*Note: Values in bold numbers show the parameters with high loadings.

The performance of magnesium oxide, half-burnt dolomite, and iron oxide was observed by the percentages of As removal from the soil samples. At 1% adsorbent added, magnesium oxide removed 73, 66, and 31% of As leaching for soil samples A, D, and F, respectively, which were averaged at 57%. Meanwhile, those of half-burnt dolomite were 66, 57, and 36%, and the average value accounted for 53%. In addition, As was also adsorbed by 72, 63, and 42% for samples A, D, and F, respectively, at 1%

iron oxide added, which were calculated at 59% on average. The average calculations were also applied in cases of 0.2 and 0.5% of adsorbent added. Magnesium oxide, half-burnt dolomite, and iron oxide removed 23, 24, and 17% of As leaching on average, respectively, at 0.2% adsorbent added. Similarly, at 0.5% adsorbent added, 45, 41, 47% of As leaching on average were adsorbed by magnesium oxide, half-burnt dolomite, and iron oxide, respectively. When the shield-tunneling machine works at the site, the excavated soils tend to mix together. Thus, the calculation for the average values is applicable. The average values of As adsorption among three kinds of adsorbents are almost similar, regardless of the doses of the adsorbents added. Therefore, the performance of magnesium oxide, half-burnt dolomite, and iron oxide was almost the same.

#### ***4.3.4 Changes in properties of soil samples with and without adsorbents***

Changes in the chemical bonding patterns of soil samples with and without adsorbents were characterized by ATR-FTIR as shown in Fig. 4.14. Two absorption bands at  $465\text{ cm}^{-1}$  and  $1,632\text{ cm}^{-1}$  are assigned to Fe—O vibration of hematite ( $\text{Fe}_2\text{O}_3$ ) (Feng et al., 2017) while absorption band at  $420\text{ cm}^{-1}$  is assigned to S—S vibration of pyrite (Tabelin et al, 2017a). The absorption bands at  $1,137$ ,  $1,070$ , and  $930\text{ cm}^{-1}$  are assigned to S—O in sulfate (Ganesan et al., 2019; Periasamy et al., 2009), which is attributed to the presence of sulfate from crystals or the result of pyrite oxidation. In addition, four absorption bands at  $780$ ,  $696$ ,  $3,700$ , and  $3,624\text{ cm}^{-1}$  are attributed to Si—O vibrations of quartz and albite (Chen et al., 2014). The findings of pyrite, quartz, and albite from the results of ATR-FTIR were well consistent with the results of XRD. In particular, there were no significant changes in chemical bonding patterns of soil samples with and without adsorbents except the absorption band at  $1,420\text{ cm}^{-1}$ , which is assigned to C—O vibration of calcite (Andersen and Brečević, 1991; Tabelin et al, 2017b) due to a significant addition of half-burnt dolomite. Changes in chemical bonding patterns of soil samples with magnesium oxide and iron oxide addition at 1% compared with soil might be lower than detection limit of the machine.

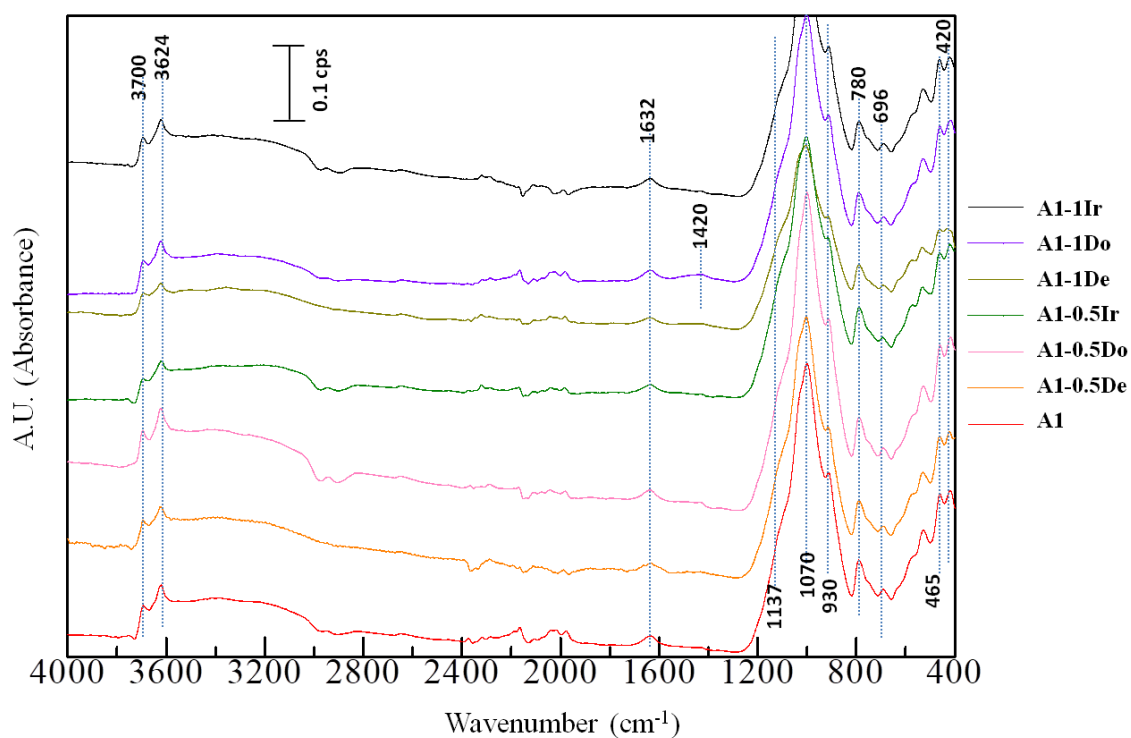


**Fig. 4.14.** The changes in ATR-FTIR of soil sample A with and without adsorbents

#### 4.3.5 Batch leaching experiments with foam reagent and coagulant

The effects of commonly used foam reagent and coagulant on As leaching are depicted in Fig. 4.15. In order to observe more accurate leaching concentrations of As, batch leaching experiments with and without foam reagent and coagulant were done in triplicate. The results showed that the leaching concentrations of As and pH with and without foam reagent and coagulant were almost the same. This indicated that leaching concentrations of As were unaffected by adding the foam reagent and coagulant.

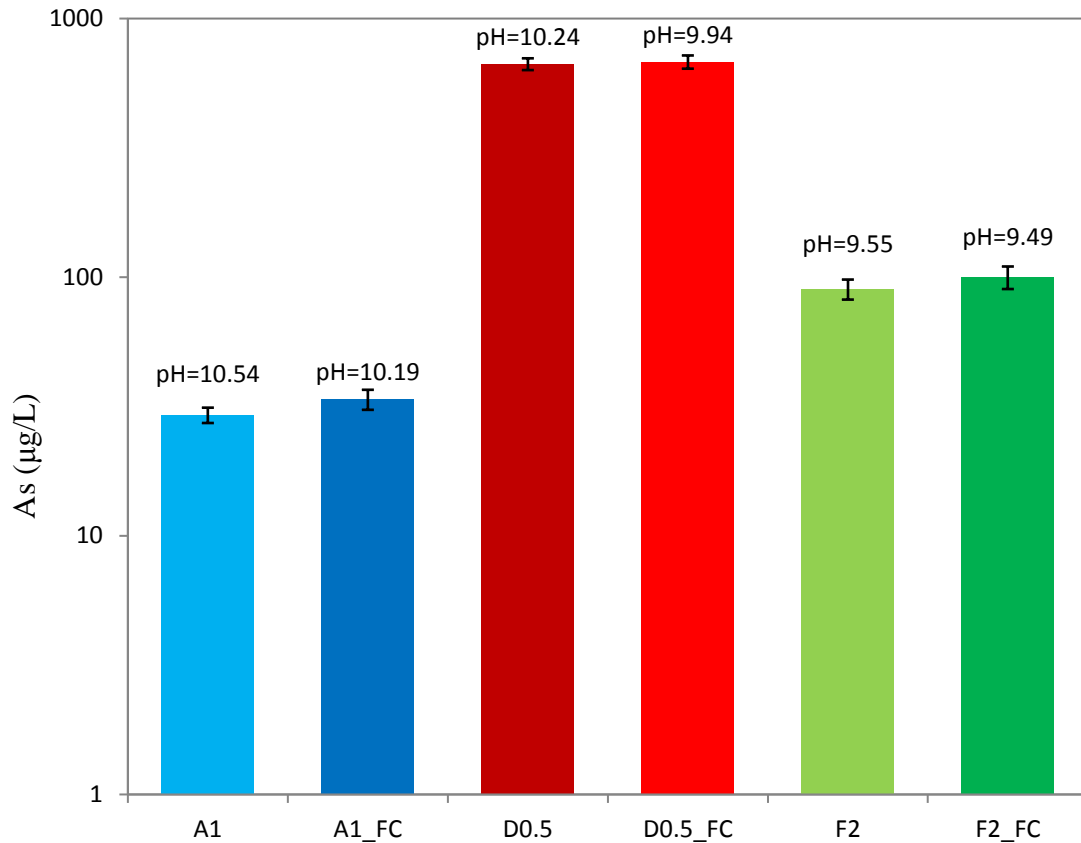


**Fig. 4.15.** Effects of foam reagent and coagulant on As leaching

\*Note: Figures above column mean pH values in the leachate

#### 4.4. Conclusions

The effects of adsorbents, foam reagent and coagulant on As leaching from soils were evaluated in the present study. Several types of experiments were done and the findings of this research can be listed as follows:

- (1) Magnesium oxide, half-burnt dolomite, and iron oxide worked effectively in restricting As leaching from shield-tunneling excavated soils.
- (2) The performance of magnesium oxide, half-burnt dolomite, and iron oxide was almost the same.
- (3) Ettringite precipitation, and adsorption/co-precipitation of As onto the Fe-surfaces and magnesium hydroxide surfaces were the major mechanisms of reduction of As leaching.

- (4) The changes in the chemical bonding of soil with half-burnt dolomite addition at the ratio of 1% compared to soil were observed by ATR-FTIR.
- (5) The leaching concentrations of As were unaffected by adding the foam reagent and coagulant.

The above results imply that As leaching is restricted by adding the adsorbents.

## References

- Andersen, F. A., Brečević, L., 1991. Infrared spectra of amorphous and crystalline calcium carbonate. *Acta Chem. Scand.*, 45(10), 1018-1024.
- Aredes, S., Klein, B., Pawlik, M., 2013. The removal of arsenic from water using natural iron oxide minerals. *Journal of Cleaner Production*, 60, 71-76.
- Ayoub, G. M., Mehawej, M., 2007. Adsorption of arsenate on untreated dolomite powder. *Journal of Hazardous Materials*, 148(1-2), 259-266.
- Banerjee, K., Amy, G. L., Prevost, M., Nour, S., Jekel, M., Gallagher, P. M., Blumenschein, C. D., 2008. Kinetic and thermodynamic aspects of adsorption of arsenic onto granular ferric hydroxide (GFH). *Water Research*, 42(13), 3371-3378.
- Bethke, C. M., Yeakel, S., 2011. *The Geochemist's Workbench® – A User's Guide to GSS, Rxn, Act2, Tact, Spec8, React, Gtplot, X1t, X2t and Xtplot*. Aqueous Solutions LLC, Urbana, Illinois.
- Chen, Y., Furmann, A., Mastalerz, M., Schimmelmann, A., 2014. Quantitative analysis of shales by KBr-FTIR and micro-FTIR. *Fuel*, 116, 538-549.
- Chen, Z., Kim, K. W., Zhu, Y. G., McLaren, R., Liu, F., He, J. Z., 2006. Adsorption (AsIII, V) and oxidation (AsIII) of arsenic by pedogenic Fe–Mn nodules. *Geoderma*, 136(3-4), 566-572.
- Drahota, P., Filippi, M., 2009. Secondary arsenic minerals in the environment: A review. *Environment International*, 35 (8), 1243-1255.
- Feng, L., Zheng, H., Gao, B., Zhang, S., Zhao, C., Zhou, Y., Xu, B., 2017. Fabricating an anionic polyacrylamide (APAM) with an anionic block structure for high turbidity water separation and purification. *RSC advances*, 7(46), 28918-28930.
- Ganesan, S., Nadarajah, S., Khairuddean, M., Teh, G. B., 2019. Studies on lauric acid conversion to methyl ester via catalytic esterification using ammonium ferric sulphate. *Renewable Energy*, 140, 9-16.



- Gupta, V. K., Saini, V. K., Jain, N., 2005. Adsorption of As (III) from aqueous solutions by iron oxide-coated sand. *Journal of Colloid and Interface Science*, 288(1), 55-60.
- Imai, N., Terashima, S., Ohta, A., Ujiie-Mikoshihara, M., Okai, T., Tachibana, Y., Togashi, S., Matsuhisa, Y., Kanai, Y., Kamioka, H., Taniguchi, M., 2004. Geochemical map of Japan. Geological Survey of Japan, AIST, 209p. Japanese with English abstract. Available at: <https://gbank.gsj.jp/geochemmap>.
- Kameda, K., Hashimoto, Y., Ok, Y. S., 2018. Stabilization of arsenic and lead by magnesium oxide (MgO) in different seawater concentrations. *Environmental Pollution*, 233, 952-959.
- Konda, T., 2001. Shield tunneling method. *Civil Engineering, Japan Society of Civil Engineering*, 39, 23-27.
- Koyama, Y., 2003. Present status and technology of shield tunneling method in Japan. *Tunnelling and Underground Space Technology*, 18, 145-159.
- Kundu, S., Gupta, A. K., 2006. Arsenic adsorption onto iron oxide-coated cement (IOCC): Regression analysis of equilibrium data with several isotherm models and their optimization. *Chemical Engineering Journal*, 122(1-2), 93-106.
- Lee, S. H., Kim, E. Y., Park, H., Yun, J., Kim, J. G., 2011. In situ stabilization of arsenic and metal-contaminated agricultural soil using industrial by-products. *Geoderma*, 161(1-2), 1-7.
- Mahedi, M., Cetin, B., Dayioglu, A. Y., 2019. Leaching behavior of aluminum, copper, iron and zinc from cement activated by fly ash and slag stabilized soils. *Waste Management*, 95, 334-355.
- Mahedi, M., Cetin, B., Dayioglu, A. Y., 2020. Effect of cement incorporation on the leaching characteristics of elements from fly ash and slag treated soils. *Journal of Environmental Management*, 253, 109720.
- Mar, K. K., Karnawati, D., Putra, D. P. E., Igarashi, T., Tabelin, C. B., 2013. Comparison of arsenic adsorption on lignite, bentonite, shale, and iron sand from Indonesia. *Procedia Earth and Planetary Science*, 6, 242-250.

- Naseri, E., Reyhanitabar, A., Oustan, S., Heydari, A. A., Alidokht, L., 2014. Optimization arsenic immobilization in a sandy loam soil using iron-based amendments by response surface methodology. *Geoderma*, 232, 547-555.
- Nath, B. K., Chaliha, C., Kalita, E., 2019. Iron oxide Permeated Mesoporous rice-husk Nanobiochar (IPMN) mediated removal of dissolved arsenic (As): chemometric modelling and adsorption dynamics. *Journal of Environmental Management*, 246, 397-409.
- Otsuka, R., 1986. Recent studies on the decomposition of the dolomite group by thermal analysis. *Thermochimica Acta*, 100(1), 69-80.
- Opiso, E. M., Sato, T., Morimoto, K., Asai, A., Anraku, S., Numako, C., Yoneda, T., 2010. Incorporation of arsenic during the formation of Mg-bearing minerals at alkaline condition. *Minerals Engineering*, 23(3), 230-237.
- Pan, Y. F., Chiou, C. T., Lin, T. F., 2010. Adsorption of arsenic (V) by iron-oxide-coated diatomite (IOCD). *Environmental Science and Pollution Research*, 17(8), 1401-1410.
- Park, Y. Y., Tran, T., Lee, Y. H., Nam, Y. I., Senanayake, G., Kim, M. J., 2010. Selective removal of arsenic (V) from a molybdate plant liquor by precipitation of magnesium arsenate. *Hydrometallurgy*, 104(2), 290-297.
- Parkhurst, D. L., Appelo, C. A. J., 1999. User's guide to PHREEQC (Version 2): a computer program for speciation, batch-reaction, one-dimensional transport, and inverse geochemical calculations. *Water-resources Investigations Report*, 99(4259), 312.
- Periasamy, A., Muruganand, S., Palaniswamy, M., 2009. Vibrational studies of Na<sub>2</sub>SO<sub>4</sub>, K<sub>2</sub>SO<sub>4</sub>, NaHSO<sub>4</sub> and KHSO<sub>4</sub> crystals. *Rasayan J. Chem.*, 2(4), 981-989.
- Salameh, Y., Albadarin, A. B., Allen, S., Walker, G., Ahmad, M. N. M., 2015. Arsenic (III, V) adsorption onto charred dolomite: charring optimization and batch studies. *Chemical Engineering Journal*, 259, 663-671.

- Schaufuß, A. G., Nesbitt, H. W., Kartio, I., Laajalehto, K., Bancroft, G. M., Szargan, R., 1998. Reactivity of surface chemical states on fractured pyrite. *Surface Science*, 411(3), 321-328.
- Siddiqui, S. I., Chaudhry, S. A., 2017. Iron oxide and its modified forms as an adsorbent for arsenic removal: A comprehensive recent advancement. *Process Safety and Environmental Protection*, 111, 592-626.
- Stefaniak, E., Biliński, B., Dobrowolski, R., Staszczuk, P., Wojcik, J., 2002. The influence of preparation conditions on adsorption properties and porosity of dolomite-based sorbents. *Colloids and Surfaces A: Physicochemical and Engineering Aspects*, 208(1-3), 337-345.
- Tabelin, C. B., Igarashi, T., 2009. Mechanisms of arsenic and lead release from hydrothermally altered rock. *Journal of Hazardous Materials*, 169(1-3), 980-990.
- Tabelin, C. B., Igarashi, T., Yoneda, T., Tamamura, S., 2013. Utilization of natural and artificial adsorbents in the mitigation of arsenic leached from hydrothermally altered rock. *Eng. Geol.*, 156, 58-67.
- Tabelin, C. B., Veerawattananun, S., Ito, M., Hiroyoshi, N., Igarashi, T., 2017a. Pyrite oxidation in the presence of hematite and alumina: II. Effects on the cathodic and anodic half-cell reactions. *Sci. Total Environ.*, 581–582, 126–135.
- Tabelin, C. B., Sasaki, R., Igarashi, T., Park, I., Tamoto, S., Arima, T., Ito, M., Hiroyoshi, N., 2017b. Simultaneous leaching of arsenite, arsenate, selenite, and selenate, and their migration in tunnel-excavated sedimentary rocks: I. column experiments under intermittent and unsaturated flow. *Chemosphere*, 186, 558–569.
- Tangviroon, P., Hayashi, R., Igarashi, T., 2017. Effects of additional layer(s) on the mobility of arsenic from hydrothermally altered rock in laboratory column experiments. *Water, Air, & Soil Pollution*, 228(5), 191.
- Tresintsi, S., Simeonidis, K., Katsikini, M., Paloura, E. C., Bantsis, G., Mitrakas, M., 2014. A novel approach for arsenic adsorbents regeneration using MgO. *Journal of Hazardous Materials*, 265, 217-225.

Yun, S. W., Park, C. G., Jeon, J. H., Darnault, C. J., Baveye, P. C., Yu, C., 2016. Dissolution behavior of As and Cd in submerged paddy soil after treatment with stabilizing agents. *Geoderma*, 270, 10-20.

Zhang, T., Zeng, X., Zhang, H., Lin, Q., Su, S., Wang, Y., Bai, L., Wu, C., 2019. The effect of the ferrihydrite dissolution/transformation process on mobility of arsenic in soils: Investigated by coupling a two-step sequential extraction with the diffusive gradient in the thin films (DGT) technique. *Geoderma*, 352, 22-32.

## CHAPTER 5

### GENERAL CONCLUSION

The present study was conducted with the main objective of evaluating the effects of pH on As leaching from the shield-tunneling excavated soils by cement addition, and proposing the As leaching countermeasures of such excavated soils. Laboratory experiments such as batch leaching tests, sequential extraction, XRD-XRF, ATR-FTIR, zeta potential, and TC/IC analyses, together with literature review were performed to achieve this goal. The general conclusions were divided into four parts, which corresponded to four chapters of this dissertation.

Chapter 1 briefly introduced As contamination of soils, geochemistry of As in environments, the removal of As, as well as shield-tunneling excavation.

Chapter 2 reviewed the recent studies related to the effects of changes in pH on As leaching. The approved results were then depicted. Therefore, the necessities of the present study were presented.

Chapter 3 were conducted to elucidate the effects of cement addition on As leaching from soils excavated from projects employing shield-tunneling method. The results indicated that leaching concentrations of As had a positive correlation with the contents of exchangeable phase As and total As when cement did not added. When cement was added, leaching concentration of As from soils depended on pH adjusted by changing the amount cement addition. The maximum leaching concentrations of As were observed at pH 10.3, and the concentrations decreased when the pH was less than 10.3 and higher than 10.3. These results indicated that As leaching was restricted by pH adjustments by considering the properties of the soils.

After identifying the effects of cement addition on As leaching, the performance of magnesium oxide, half-burnt dolomite, and iron oxide adsorbents on As leaching from the soils was evaluated and compared. In addition, the effects of commonly used foam reagent and coagulant on As leaching from the soils, which are used in cases needed for enhancing the excavation performance, were also investigated in chapter 4. The results indicated that As leaching was restricted by adding the adsorbents while

magnesium oxide, half-burnt dolomite, and iron oxide worked effectively in restricting As leaching from shield-tunneling excavated soils, and that the performance of magnesium oxide, half-burnt dolomite, and iron oxide was almost the same. Besides, the leaching concentrations of As were unaffected by adding the foam reagent and coagulant.

## ACKNOWLEDGMENT

Firstly, I would like to express my deepest gratitude to my advisor Prof. Toshifumi IGARASHI for giving me the opportunity to pursue the doctoral degree in his laboratory, continuously supporting, and guiding me throughout my Ph. D. study. His encouragement, immense knowledge, and expert advice from the initial to the final step enabled me to develop a deep understanding of my research and thesis writing as well.

Besides my principal advisor, I would like to sincerely thank the rest of my thesis committee for the past 3 years: Prof. Satoru KAWASAKI, and Associate Prof. Koichi ISOBE for their insightful comments and expert advice, which guided me to develop my research. Also, I would like to express my sincere thank to Associate Prof. Shusaku HARADA for his motivation and encouragement, and Assistance Prof. Carlito Baltazar Tabelin for his suggestion, guidance, and correction on my manuscript.

I am heartily thankful to all lectures in the Division of Sustainable Resources Engineering for providing valuable knowledge during my Ph. D. time in Japan. Moreover, it is a pleasure to thank all members of e<sup>3</sup> family for their warm welcome since the first day I came here.

To all fellow lab-mates in the Laboratory of Groundwater and Mass Transport, thank you very much for guiding me to use the machine. I could not be able to conduct experiments without your assistance. In particular, your kindness and your friendship warmed me up. I feel like staying in my home country. I could not forget the crazy parties that we enjoyed together.

Unforgettably, I am appreciated to my scholarship sponsor JICA under Asian University Network, Southeast Asia Engineering Education and Development Network (AUN/SEED-Net) Program for its financial and academic support. Without this program, I would not be able to pursue a Ph.D. degree in the Division of Sustainable Resources Engineering, Hokkaido University, Japan.

Moreover, it is unforgettable to extend my acknowledgment to all people who I have failed to mention above for their kind help, and support during my Ph.D. life.

Finally, I would like to deeply thank my Dad and my Mom who have managed to bring me up all the way. They have devoted all their life to me.